ELSEVIER

Coordination Chemistry Reviews
184 (1999) 3–66

COORDINATION CHEMISTRY REVIEWS

Metal complexes as diagnostic tools

David E. Reichert, Jason S. Lewis, Carolyn J. Anderson *

Mallinckrodt Institute of Radiology, Washington University School of Medicine, 510 South Kingshighway, Campus Box 8225, St. Louis, MO 63110, USA

Received 20 November 1997

Contents

* Corresponding author. Tel.: +1-314-3628427; fax: +1-314-3629940.
E-mail address: andersoncj@mirlink.wustl.edu (C.J. Anderson)

PII: S0010-8545(98)00207-0

Abstract

This review summarizes some of the developments of metal complexes and metal-complex-bioconjugates for the diagnosis of disease states that have occurred over the past 10 years. The diagnostic imaging modalities discussed are gamma scintigraphy, positron emission tomography (PET) and magnetic resonance imaging (MRI). Metal complexes are utilized in all three imaging modalities to image a broad array of diseases, including heart disease, brain disorders and cancer. There are a wide variety of different radiometals that have been utilized in the synthesis of coordination compounds for gamma scintigraphy and PET, and

these will be discussed individually. The field of metal-complex-bioconjugate chemistry is covered extensively, describing radiometals labeled to biomolecules such as receptor ligands for diseases such as neurological disorders and cancer. A section is devoted to the development of coordination compounds for MRI enhancement agents, and specifically details the agents that have been evaluated in vivo, both in animal models and in humans. Overall, the goal of this review is to demonstrate the significant progress made in the field of coordination chemistry as it applies to the development of diagnostic imaging agents.

Keywords: Metal complexes; Disease states; Diagnostic imaging agents

1. Introduction

1.1. Coordination chemistry as it applies to diagnostic imaging

The use of metal complexes in therapy and diagnostic imaging is increasing. Throughout history, both ancient and modern, metals and metal compounds have been used in medicine to treat a variety of ailments. In the last century, metal complexes were used to treat diseases ranging from syphilis (organoarsenic compounds) to cancer (platinum anti-tumor drugs) to arthritis (gold compounds). The use of metal complexes as diagnostic agents is a relatively new area of medical research, and has flourished during the last 40 years. The end of World War II heralded the use of nuclear technology for medical purposes, opening up nuclear reactors, accelerators and cyclotrons for medical isotope production. The first isotope used in medicine was iodine-131, which in 1946 was used to treat thyroid cancer. In 1959, Brookhaven National Laboratory developed the $^{99}Mo/^{99m}Tc$ generator, and in 1964 the first ^{99m}Tc radiotracers were developed at Argonne National Laboratory. Currently, ^{99m}Tc is the most widely used radionuclide for diagnostic imaging. The advent of ^{99m}Tc radiopharmaceuticals began the study of coordination chemistry as it relates to diagnostic imaging. Today, there are a wide variety of radiometals and radiometal complexes used in gamma scintigraphy and positron emission tomography (PET).

An even more recent development is the use of paramagnetic metal complexes for enhancing contrast of magnetic resonance imaging (MRI). There are now a number of non-radioactive metal complexes used as MRI contrast agents. The purpose of this review is to highlight the new developments in applying metal complex chemistry to gamma scintigraphy, PET and MRI over the last 10 years.

1.2. Diagnostic modalities

Imaging modalities widely used in radiology include gamma scintigraphy, PET and MRI. Gamma scintigraphy requires a radiopharmaceutical containing a nuclide that emits gamma (γ) radiation (Table 1) and a gamma camera or a single photon emission computed tomography (SPECT) camera capable of imaging the

patient injected with the gamma emitting radiopharmaceutical. PET requires a radiopharmaceutical labeled with a positron-emitting radionuclide (β^+) (Table 2) and a PET camera for imaging the patient. Positron decay results in the emission of two 511 keV photons at ca. 180° apart. PET scanners contain a circular array of detectors to detect specifically the 511 keV photons emitted in opposite directions. MRI exploits the differences in relaxation rates of water protons in tissues, translating them into three-dimensional anatomical information.

Metal complexes are used in all three imaging modalities, but in a clinical situation are most widely applied to gamma scintigraphy. For gamma scintigraphy and PET, radiopharmaceuticals labeled with metal radionuclides are injected into patients to diagnose medical problems such as cancer, infection, kidney and liver abnormalities and cardiological and neurological disorders. The biological distribution of radiopharmaceuticals is generally governed by two factors: (1) perfusion (or blood flow) and (2) specific biochemical processes such as receptor/antigen binding. MRI is generally used to generate anatomical information; however, in the last 10 years, MRI has demonstrated impressive capabilities for perfusion imaging. At the present time, the capabilities for MRI imaging of biochemical processes such as receptor binding have not yet been demonstrated.

1.3. Desirable properties of metal radionuclides

Tables 1 and 2 show the wide variety of gamma and positron emitting radiometals, their decay characteristics and methods of production. In designing radiometal-based radiopharmaceuticals, important factors to consider include the half-life of the radiometal, the mode of decay, and the cost and availability of the

Table 1
Gamma-emitting radionuclides

Isotope	$T_{1/2}$ (h)	Production methods	Decay mode	E_γ (keV)	$E_{\beta-}$ (keV)	Ref.
^{67}Cu	62.01	Accelerator, ^{67}Zn(n,p)	β^- (100%)	91, 93, 185	577, 484, 395	[121,340]
^{67}Ga	78.26	Cyclotron	EC (100%)	91, 93, 185, 296 388		[340]
^{90}Y	64.06	^{90}Sr/^{90}Y generator	β^- (72%)		2288	[340]
^{99m}Tc	6.0	^{99}Mo/^{99m}Tc generator	IT (100%)	141		[340]
^{111}In	67.9	Cyclotron, ^{111}Cd(p,n)^{111}In	EC (100%)	245, 172		[340]
^{186}Re	90.6	Reactor, ^{185}Re(n, γ) ^{186}Re	β^- (92%) EC (8%)	137	1071, 934	[340]
^{188}Re	16.98	^{188}W/^{188}Re generator	β^- (100%)	155	2116, 1965	[340]

Table 2
Positron-emitting radionuclides

Isotope	$T_{1/2}$ (h)	Methods of production	Decay mode	$E_{\beta+}$(keV)	Ref.
^{55}Co	17.5	Cyclotron, ^{54}Fe(d,n)^{55}Co	β^+(77%) EC (23%)	1513, 1037	[341,342]
^{60}Cu	0.4	Cyclotron, ^{60}Ni(p,n)^{60}Cu	β^+(93%) EC (7%)	3920, 3000 2000	[119,121,341]
^{61}Cu	3.3	Cyclotron, ^{61}Ni(p,n)^{61}Cu	β^+(62%) EC (38%)	1220, 1150 940, 560	[119,121,341]
^{62}Cu	0.16	^{62}Zn/^{62}Cu generator	β^+(98%) EC (2%)	2910	[121,341]
^{64}Cu	12.7	Cyclotron, ^{64}Ni(p,n)^{64}Cu	β^+(19%) EC (41%) β^- (40%)	656	[120,121,341]
^{66}Ga	9.5	Cyclotron, ^{63}Cu(α,nγ)^{66}Ga	β^+(56%) EC (44%)	4150, 935	[341]
^{68}Ga	1.1	^{68}Ge/^{68}Ga generator	β^+(90%) EC (10%)	1880, 770	[341,343]
^{86}Y	14.7	Cyclotron, ^{86}Sr(p,n)^{86}Y	β^+(33%) EC (66%)	2335, 2019 1603, 1248 1043	[341,344]
^{94m}Tc	0.88	Cyclotron, ^{nat}Mo(p,n)^{94m}Tc	β^+(72%) EC (28%)	2470	[341,345]

isotope. For diagnostic imaging, the half-life of the radionuclide must be long enough to carry out the desired chemistry to synthesize the radiopharmaceutical, but short enough to limit the dose to the patient. Radiometals for coordination complex-based radiopharmaceuticals used in PET and gamma scintigraphy range in half-life from about 10 min (^{62}Cu) to several days (^{67}Ga). The desired half-life is dependent upon the time required for the radiopharmaceutical to localize in the target tissue. For example, heart or brain perfusion-based radiopharmaceuticals require shorter half-lives, since they reach the target quickly, whereas tumor-targeted radiopharmaceuticals often take longer to reach the target for optimal target to background ratios to be obtained.

For diagnostic imaging in nuclear medicine, the majority of radionuclides decay primarily by gamma emission, since gamma scintigraphy is the most commonly used modality. Radionuclides used in PET decay by positron emission. The use of radiopharmaceuticals for therapeutic applications (alpha (α) or beta (β^-) emitters) is increasing, and many of these radionuclides also emit gammas or positrons for application in both therapy and imaging. The energy of the gamma photons is of great importance, since most gamma cameras are designed for specific energy windows, generally in the range of 100–200 keV. Radionuclides that decay with gamma energies either higher or lower than this range may not produce images of sufficient quality and are generally not used routinely.

Another important factor in choosing radionuclides for diagnostic imaging is their cost and availability. Radionuclide generators are considered ideal, since they consist of a longer-lived parent isotope that decays to a shorter-lived daughter radionuclide. The daughter can be separated easily from the parents by either ion exchange chromatography (the more common method) or solvent extraction. If the parent isotope is of relatively low cost, then even small hospitals can have a ready supply of the daughter radionuclide as needed. A few radiometals used for radiopharmaceuticals for gamma scintigraphy or PET are produced by a nuclear reactor. The most important of these is ^{99}Mo used to generate ^{99m}Tc. These isotopes are generally affordable, since nuclear reactors have the capability to produce many isotopes at one time. Other radiometals are accelerator or cyclotron-produced, which is probably the most expensive mode of production, since the cyclotron or accelerator can only produce one isotope at a time.

1.4. Properties of metal complexes

Designing metal complex based imaging agents requires correlating aspects of the coordination chemistry with in vivo behavior. Factors to consider include the redox properties, stability, stereochemistry, charge and lipophilicity of the metal complex. The target organ or tissue to be imaged will dictate the desired characteristics of the metal complex. For example, it is known that negatively charged compounds tend to clear through the kidneys, many positively charged ions accumulate in the heart, and an overall neutral complex is required for crossing the blood–brain barrier. Lipophilic complexes will generally have more uptake in the liver or in fatty tissues. Stereochemistry is important when targeting complexes to specific receptors. An-

other important factor is complex stability; while thermodynamic stability of non-radioactive metal complexes can help predict in vivo behavior, it is often not indicative of in vivo stability. There are few absolute rules, and it is a continuous learning process to correlate the characteristics of the metal complex to the in vivo behavior. All of these factors will be discussed for the various radiopharmaceuticals and MRI contrast agents.

1.5. Organization of the review

This review is organized into two major sections: metal-based radiopharmaceuticals and MRI contrast agents. The first part of the review will discuss radiopharmaceuticals based on their radiometal, and this will then be followed by a section on radiometal-labeled bioconjugates. The greatest attention has been given to new agents developed in the last 10 years that have been evaluated in vivo and that have not already been thoroughly reviewed. The second part of the review will focus on MRI contrast agents, and in particular agents that have been or are currently in clinical trials. A major focus will be on gadolinium complexes, followed by sections on manganese and iron compounds. A smaller section is devoted to bioconjugate MRI contrast agents.

2. Metal-based radiopharmaceuticals

2.1. Technetium

Technetium is the only transition metal that has no stable isotopes, and the longest lived isotope, ^{99}Tc ($T_{1/2} = 2.1 \times 10^5 y$), was discovered in 1937 by Perrier and Segre. Technetium-99m ($T_{1/2} = 6.02$ h, E_γ 140 keV) dominates the field of diagnostic nuclear medicine, accounting for over 80% of diagnostic scans performed in US nuclear medicine departments [1]. Technetium radiopharmaceuticals are used routinely for the imaging of diseased tissues in the human body, e.g. heart, brain, kidney and bone. Its chemistry and radiochemistry has received wide attention over the last few decades due to its ideal characteristics as a diagnostic radioisotope. ^{99m}Tc presents an isotope with a gamma emission suitable for SPECT imaging, an economic and straightforward production route (^{99}Mo/^{99m}Tc generator in the form of $^{99m}TcO_4^-$) and a chemistry that is both versatile and extensive. Its half-life permits longer radiopharmaceutical preparation time than many other useful metal isotopes yet the half-life is short enough to minimize radiation dose to the patient.

The coordination chemistry of technetium is diverse as a consequence of the range of available oxidation states (-1 to $+7$), a wide number of coordination geometries, and its ability to bind to a large range of donor ligands to fulfill its coordination requirements. This flexibility can also be a hindrance when considering synthetic methods as well as the ultimate fate of the coordination compounds in vivo. The use of ^{99m}Tc has been reviewed exhaustively over the last few years, in terms of its current use in metal-essential radiopharmaceuticals [2–4], its coupling

chemistry to both small and large biomolecules [5–10], and its coordination chemistry [11–14]. Many more reviews, commentaries, texts and articles exist on the subject of technetium in radiopharmaceutical chemistry. In this review article the authors wish to focus on four new and interesting areas in the development of technetium radiopharmaceuticals: (1) the use of lipophilic, cationic complexes to detect multi-drug resistance (MDR) (Section 2.1.1); (2) ^{99m}Tc complexes to identify hypoxic tissue (Section 2.1.2); (3) the use of technetium essential compounds to bind and image dopamine receptors (Section 2.8.3); and (4) the binding of technetium to peptides and proteins to image disease (Sections 2.8.4 and 2.8.5).

2.1.1. ^{99m}Tc-labeled MDR imaging agents

In chemotherapy, drug resistance presents a significant barrier to successful management of cancers in humans. Resistance can be correlated to over-expression of the multi-drug resistance (MDR) genes [15,16] either before or after beginning chemotherapy. P-glycoprotein (Pgp) is a 170 kDa transmembrane glycoprotein encoded by the MDR1 gene and is one of the active transport system proteins responsible for resistance of some tumor cells to multiple chemotherapeutic agents [17,18]. Pgp recognizes a variety of apparently unrelated compounds and acts as an efflux pump working in an energy dependent manner. More recently a MDR associated protein (MRP) of about 190 kDa has been described [19].

Lipophilic cations enter and accumulate in cells by passive diffusion, specifically within mitochondria, as a result of the electrical potential gradient across the respective membranes in actively metabolizing cells [20]. Complexes with these properties can also act as substrates for Pgp and hence can be used to image functional expression of MDR in tumors in vivo [21] and modulation of resistance prior to a chemotherapy regime.

Technetium lipophilic cations have been investigated as imaging markers for MDR. The primary technetium compound of interest is the ^{99m}Tc-complex of 2-methoxyisobutaneisonitrile [22] (^{99m}Tc–SESTAMIBI) (Fig. 1v). ^{99m}Tc–SESTAMIBI is an established radiopharmaceutical for myocardial perfusion imaging (Cardiolite™, Dupont) but has been investigated also for oncological applications [23]. The complex consists of six identical alkyl isonitrile ligands stabilizing the Tc(I) metal core in an octahedral array. The lipophilic, monocationic complex is extremely stable in vivo and contains no ionizable functional groups. ^{99m}Tc–SESTAMIBI is recognized and transported by the MDR1 Pgp protein [24–28], it has been clinically evaluated and has been shown to be an efficient agent for functional imaging of Pgp expression in breast cancer patients [29] and patients with refractory cancer [30].

An extensive array of analogous aromatic isonitrile Tc(I) complexes have been investigated and reported also [31] (Fig. 1). This exhaustive range of complexes have been synthesized to contain functionalities (e.g. methoxyaryl moieties) common to a wide range of established MDR transport substrates and modulators.

The interest in lipophilic cationic complexes of technetium as Pgp substrates has led to the investigation of two more ^{99m}Tc-radiopharmaceuticals. TechneCard™ (^{99m}Tc-Q12) (Mallinckrodt Medical) (Fig. 2) contains a monophosphine and a

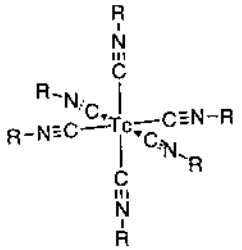

R =

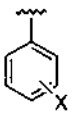

X =

a 4-methoxy
b 3,4-dimethoxy
c 3,5-dimethoxy
d 3,4,5-trimethoxy
e 3,4-methylenedioxy
f 4-cyano
g 4-acetyl
h 3-acetamido
i 3-nitro
j 4-nitro
k 3-hydroxymethyl
l 2-methoxy-5-nitro
m 5-methoxy-2-methyl-4-nitro

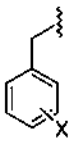

n 4-methoxy
o 3,4-dimethoxy
p 3,5-dimethoxy
q 3,4,5-trimethoxy
r 3,4-methylenedioxy

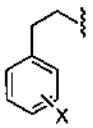

s 4-methoxy
t 3,4-dimethoxy
u 3,4,5-trimethoxy

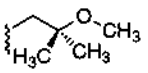

v SESTAMIBI

Fig. 1. Aromatic isonitrile Tc(I) complexes investigated for recognition and transport by the MDR1 Pgp protein.

Schiff-base [32,33]. This compound is a modification of the first such agent evaluated in humans, *trans*-[$^{99m}Tc^{III}(acac_2en)(PMe_3)_2]^+$. It belongs to a series of non-reducible Tc(III) complexes containing an $N_2O_2P_2$ donor atom set, modified to enhance biodistribution properties. TechneCard™ contains the complex of the general formula *trans*-[$^{99m}Tc^{III}(L)(P)_2]^+$, where L is the Schiff-base dianion 1,2-bis[-dihydro-2,2,5,5-tetramethyl-3(2H)-furano-4-methyleneamino]ethane and P is tris(3-methoxy-1-propyl)phosphine. This compound may not be as efficient as the primary compound ^{99m}Tc–SESTAMIBI as a substrate for Pgp [34]; however,

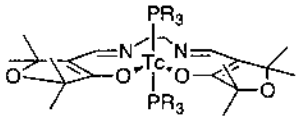

R = $(CH_2)_3OCH_3$ Technecard™

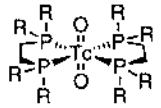

R = $(CH_2)_2OC_2H_5$ Myoview™

Fig. 2. Lipophilic Tc(III) (TechneCard™) and Tc(V) (Myoview™) complexes recognized by the Pgp protein.

further investigations are currently underway into this series of non-reducible Tc(III) cations [35].

Another radiopharmaceutical evaluated as a substrate for Pgp is Myoview™ (Amersham) (Fig. 2), a tetrofosmin complex of ^{99m}Tc. Tetrofosmin is a recently developed bis(diphosphine) ligand which forms a cationic, lipophilic complex with ^{99m}Tc, $[^{99m}Tc^{V}(\text{tetrofosmin})_2O_2]^+$ [36,37]. This compound demonstrated rapid heart uptake and rapid blood clearance, comparable to that of ^{99m}Tc–SESTAMIBI, but with improved renal clearance and less hepatobiliary excretion [37]. The complex is an analogue of *trans*-$[Tc^{V}O_2(DMPE)_2]^+$ in which the pendant phosphorous groups have been modified to enhance its biokinetics. The compound contains the dioxo–Tc(V) core, which is kinetically blocked from undergoing in vivo reduction. ^{99m}Tc–tetrofosmin has been shown in vitro to be an efficient substrate for Pgp [38]. Although no clinical data is available at present for this compound as a substrate for Pgp, it may be more suitable than ^{99m}Tc–SESTAMIBI as a consequence of its clearance properties, offering the possibility of imaging abdominal tumors.

The use of lipophilic, cationic, hydrophobic technetium complexes as substrates for Pgp has now been firmly established. The modification and enhancement of current radiopharmaceuticals has led to the identification of a number of candidates as described above. It seems reasonable to assume that many more technetium compounds, and indeed cationic, lipophilic compounds of other metals (see Section 2.6.2), will be utilized in functional imaging of multi-drug resistance.

2.1.2. ^{99m}Tc-labeled hypoxia imaging agents

Myocardial infarction, acute cerebral injury and tumors can have areas of hypoxic (oxygen deficient) tissue that are important to identify for determining the optimal treatment regime. For example, in tumors a strong negative correlation between pretreatment tumor hypoxia and response to radiotherapy has been reported [39]. The pretreatment tumor hypoxia is independent of tumor size and is considered a prognostic indicator of poor clinical outcome following radiotherapy.

Designing a coordination complex that will be trapped selectively in hypoxic tissue depends on a fine balance between redox potential and cell uptake. The

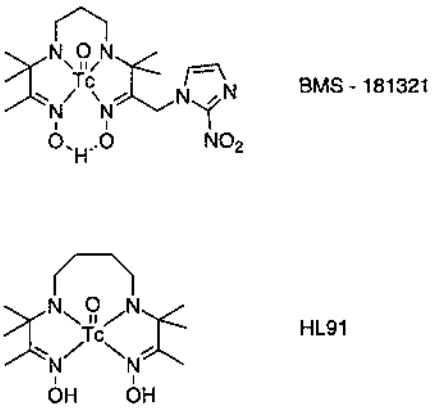

Fig. 3. ^{99m}Tc-labeled hypoxia imaging agents.

selective trapping of a complex requires that its reduction potential is such that the complex is reduced in hypoxic tissue but not reduced in normoxic tissue. Nitroimidazoles have been investigated as markers for hypoxic tissue and a ^{99m}Tc labeled nitromidazole complex BMS-181321 (Fig. 3) has been investigated as a possible agent for the delineation of hypoxic tissue in vivo. The single-crystal X-ray structure of this neutral complex shows a five-coordinate Tc(V) center of square–pyramidal geometry containing the oxo-group in the apical position [40,41]. Electrochemical results from the same paper [41] quote a redox potential of -1480 mV which is 10 mV more positive than that of misonidazole, the gold standard of hypoxia targeting agents. BMS-181321 has been used with some success to identify hypoxia in the heart [42–45] and in tumors [46].

The ^{99m}Tc compound, ^{99m}Tc-HL91, has demonstrated increased uptake in hypoxic and low-flow ischemic myocardium [47]. The compound is similar to BMS-181321 in its donor atom set (N_4) but does not contain a nitromidazole moiety (Fig. 3). Other ^{99m}Tc complexes have been investigated which include the structurally unrelated Schiff-base/monophosphine complex TechneCard™ described above [48]. Any coordination compound that can traverse the cell membrane and has a redox potential that will ultimately trap the radionuclide selectively in hypoxic cells may have clinical usefulness in the determination of hypoxia in tissue.

2.2. Rhenium

Rhenium is the group VII congener of technetium and the chemical similarity between the two elements stems from the lanthanide contraction observed for second and third row transition metals [49]. The coordination compounds of the two elements are similar in terms of size, geometries, dipole moments, lipophilicity, etc. and as a consequence non-radioactive rhenium has often been used as an alternative to ^{99}Tc in preliminary investigations. One major difference between analogous Tc and Re complexes is that their redox potentials can differ signifi-

cantly, with technetium complexes being more easily reduced. This has practical consequences for nuclear medicine since reduced rhenium radiopharmaceuticals have a greater tendency to reoxidize back to perrhenate (ReO_4^-) than do the analogous technetium complexes to pertechnetate (TcO_4^-). The relationship between rhenium and technetium chemistry in terms of their use in nuclear medicine is discussed in a 1986 publication [50]. The isotopes of rhenium are primarily used as therapeutic agents, and as such have lead to the development of therapeutic ^{186}Re ($T_{1/2} = 3.78$ d, $E_{\beta-} = 1.07$, 0.93 MeV) and ^{188}Re ($T_{1/2} = 16.9$ h, $E_{\beta-} = 2.1$ MeV) drugs based on ^{99m}Tc imaging agents. The γ-emission following β^- decay in ^{186}Re ($E_\gamma = 137$ keV) and ^{188}Re ($E_\gamma = 155$ keV) allows imaging which is useful when considering the ultimate fate and dosimetry of the radiopharmaceutical used for a therapeutic application.

The treatment of bone metastases has been the major use of rhenium complexes to date. ^{186}Re has been complexed to hydroxyethylidene diphosphonate (HEDP) [50], which localizes in bone by bridging hydroxyapatite. ^{186}Re–HEDP is an effective palliative treatment of metastatic bone pain and is currently under clinical investigation [51,52]. There have also been a number of publications on rhenium agents which are based on the attachment of the radionuclide of choice to biomolecules. These compounds will be discussed in Section 2.8.2.

2.3. Gallium

2.3.1. Gallium (III) chemistry

The coordination, analytical and radiopharmaceutical chemistry of gallium has been reviewed [53–57]. The most prevalent oxidation state of gallium in aqueous solution is +3, and this is the oxidation state most relevant to radiopharmaceutical chemistry. The complexation of Ga(III) is dominated by ligands containing oxygen, nitrogen and sulfur donor atoms. Gallium has well established coordination numbers of 3, 4, 5, and 6 depending on the ligand; generally, six-coordinate Ga(III) complexes are most stable in vivo. The ionization potential, ionic radii and coordination number of Ga(III) are very similar to that of Fe(III), because Fe(III) has a half-filled 3d orbital, similar to Ga(III) which has a filled 3d orbital.

2.3.2. Isotopes of gallium used in diagnostic imaging

There are three gallium radioisotopes with decay characteristics that are suitable for either gamma scintigraphy or PET imaging. ^{67}Ga ($T_{1/2} = 78$ h) is cyclotron-produced, decays by γ-emission, and is used in gamma scintigraphy. ^{67}Ga was first produced for human use in 1953 [58]. ^{68}Ga ($T_{1/2} = 68$ min) is produced from the $^{68}Ge/^{68}Ga$ generator [59], decays by 89% β^+-emission, and is used in PET imaging. The long half-life of the parent isotope, ^{68}Ge ($T_{1/2} = 280$ days) gives this generator a shelf-life of 1–2 years, allowing PET imaging at facilities without an on-site cyclotron. ^{66}Ga ($T_{1/2} = 9.4$ h) is a cyclotron produced β^+-emitting radioisotope and has been used in a small number of studies evaluating the utility of a medium half-life β^+-emitting gallium radionuclide for labeling slower clearing biomolecules [60,61]. Radiopharmaceuticals labeled with ^{67}Ga and ^{68}Ga will be discussed.

There are two requirements for using gallium complexes as radiopharmaceuticals: they should be stable to hydrolysis (formation of complexes with OH^-), and they should be more stable than the Ga(III)–transferrin complex. In aqueous solution, free hydrated Ga(III) is stable only under acidic conditions, with insoluble $Ga(OH)_3$ forming as the pH is raised. Between pH 3 and about 9.5, insoluble $Ga(OH)_3$ is the primary species, whereas above pH 9.6, the soluble gallate ion ($Ga(OH)_4^-$) forms. In the preparation of Ga(III) coordination complexes, ligand exchange is often necessary since the precipitation of $Ga(OH)_3$ occurs more rapidly than complexation with ligands that bind Ga(III) at a slower rate. For example, $GaCl_3$ is generally complexed first with a weakly coordinating ligand such as acetate or citrate, and then this Ga(III) species is used to prepare coordination complexes of higher stability.

Gallium radiopharmaceuticals must also be resistant to exchange with the plasma protein transferrin. The large formation constant of Ga(III)–transferrin ($\log K_1 = 20.3$) [62] and the high plasma concentration of this protein (0.25 g/100 ml) thermodynamically favor the in vivo exchange of many Ga(III) complexes with transferrin. The majority of radiogallium complexes used as radiopharmaceuticals have very high thermodynamic stability or are kinetically stable to exchange with transferrin in vivo. Ligands that form highly stable complexes are generally multidentate and contain carboxyl, amino or thiol groups.

2.3.3. ^{67}Ga- and ^{68}Ga–citrate

There is one clinically used radiopharmaceutical that takes advantage of the in vivo exchange of Ga(III) with transferrin. ^{67}Ga-labeled citrate was first used in tumor imaging nearly 30 years ago [63], and a few years later researchers determined that the ^{67}Ga was actually binding transferrin in vivo [64]. Today, ^{67}Ga–citrate/transferrin remains a widely used radiopharmaceutical for the clinical diagnosis of certain types of neoplasms, such as Hodgkin's disease, lung cancer, non-Hodgkin's lymphoma, malignant melanoma and leukemia. The mechanism of ^{67}Ga–citrate/transferrin uptake into tumors has long been disputed. The current theory is that the ^{67}Ga–transferrin complex binds to the transferrin receptor present on tumor cells, and is then incorporated into the cell by receptor-mediated endocytosis [65].

^{68}Ga labeled citrate/transferrin has also been used in diagnostic imaging, but due to the much shorter half-life of ^{68}Ga than ^{67}Ga, the disease states studied are very different. For example, ^{68}Ga–transferrin has been used to quantify pulmonary vascular permeability using PET [66], where ^{68}Ga–transferrin is taken up in the lungs immediately after injection. The use of PET allows quantification capabilities that are not possible with ^{67}Ga and gamma scintigraphy.

2.3.4. ^{68}Ga-labeled myocardial imaging agents

Because of the convenient half-life of ^{68}Ga, and the fact that it is generator-produced and therefore more widely available, considerable interest lies in the development of ^{68}Ga-labeled myocardial, cerebral and tumor targeting agents. During the last 10 years, there have been significant advances in the development of ^{68}Ga-la-

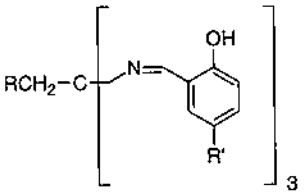

Ligand	R	R'
H_3[(5-MeOsal)$_3$tame]	H	-OCH_3
H_3[(sal)$_3$tame-O-n-Bu]	-$O(CH_2)_3CH_3$	H
H_3[(sal)$_3$tame -O-iso-Bu]	-$OCH_2CH(CH_3)_2$	-H
H_3[(5-MeOsal)$_3$tame-O-sec-Bu]	-$OCH(CH_3)CH_2CH_3$	-H
H_3[(5-MeOsal)$_3$tame-O-nPr]	-$O(CH_2)_2CH_3$	-OCH_3

Fig. 4. Ligands evaluated as ^{68}Ga-labeled myocardial imaging agents in an animal model.

beled myocardial imaging agents. Lipophilic Ga(III) complexes, both neutral and cationic, have been shown to localize in the heart. Uncharged, lipophilic Ga(III) complexes of 1,1,1-tris-(5-methoxysalicylaldiminomethyl)ethane [5-MeO(sal)$_3$tame] and other 1,1,1-tris-(alkoxysalicylaldiminomethyl)ethane derivatives [(ROsal)$_3$tame] were investigated as ^{68}Ga myocardial imaging agents with limited success [67,68]. Green and coworkers followed up on these agents with more lipophilic tris(salicylaldimine) agents containing alkoxy substituents on the ethane backbone of the triamine framework, (Fig. 4) [69]. Although these agents had increased uptake in the heart and higher heart:blood ratios, their increased lipophilicity resulted in high accumulation of the tracer in the liver. Tsang and coworkers prepared a series of hexadentate bis(salicylaldimine) ligands that formed lipophilic cationic Ga(III) complexes, and found that one of the complexes, ^{68}Ga–[(4,6-

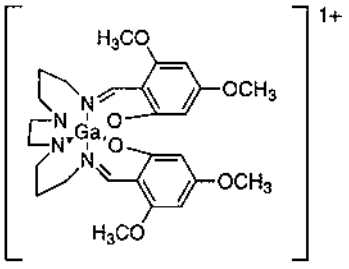

Ga((4,6-MeO_2sal)$_2$BAPEN)

Fig. 5. Lipophilic cationic Ga(III) complex exhibiting significant myocardial uptake in an animal model.

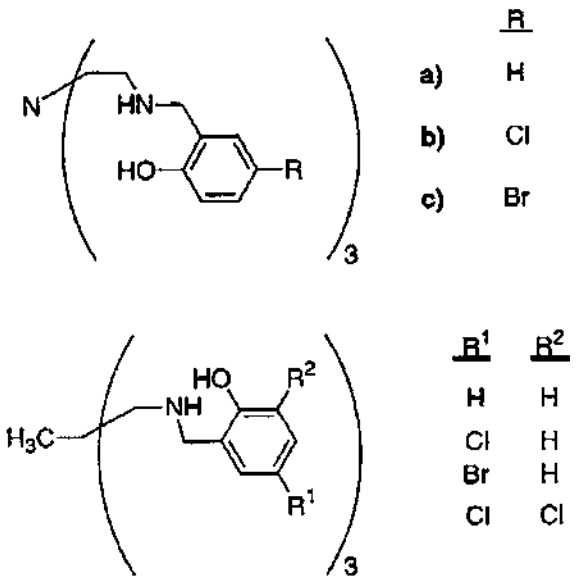

Fig. 6. Tripodal amine phenol ligands for Ga(III) which form both either cationic or neutral species.

$MeO_2sal)_2BAPEN]^+$ (Fig. 5), exhibited significant myocardial uptake and retention over the neutral salicylaldimine ligands [70,71].

Liu and coworkers reported on two series of tripodal amine phenol ligands for Ga(III) (Fig. 6). One set of ligands had an N_4O_3 backbone and formed cationic complexes with Ga(III) [72]. The other series had three chelating arms bridged by a carbon atom (N_3O_3), formed neutral complexes with Ga(III), and were considered more pre-organized and possibly more stable [73]. Both series of ligands formed distorted octahedral complexes and have potential as myocardial imaging agents. To date, no stability or in vivo studies have been reported.

Zhang et al. evaluated a series of neutral, highly lipophilic Ga(III) complexes of 1-aryl-3-hydroxy-2-methyl-4-pyridinones (Fig. 7) and found heart uptake of these complexes in rabbit and dog models [74]. Although these complexes were only stable a short time in vivo, the complexes were stable long enough for a first pass extraction by the heart, and for one of the complexes, the brain.

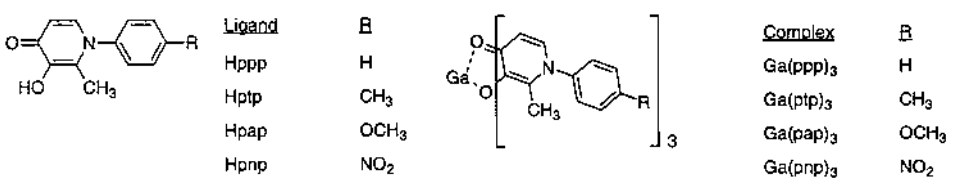

Fig. 7. Lipophilic 1-aryl-3-hydroxy-2-methyl-4-pyridinones and their Ga(III) complexes.

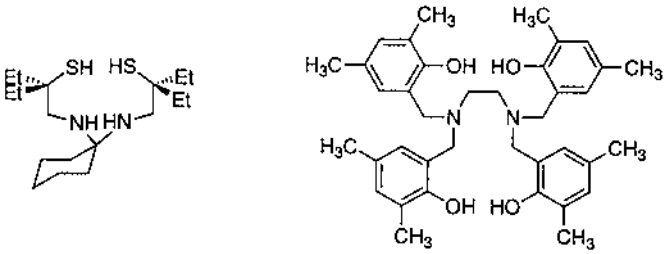

a) BAT-TECH b) THM_2BED

Fig. 8. (a) The N_2S_2 ligand BAT–TECH whose Ga(III) complex showed significant myocardial uptake in an animal model. (b) The hexacoordinate N_2O_4 ligand THM_2BED which showed both heart and brain uptake in rats.

Other ligands that have been evaluated for myocardial imaging include a ^{68}Ga complex with a four-coordinate N_2S_2 ligand, (BAT–TECH) (Fig. 8a) [75,76]. This ^{68}Ga complex showed significant uptake in the heart; however, the activity washed out over time, and the blood activity remained constant after 30 min. Another complex evaluated as a heart agent is the ^{68}Ga complex of THM_2BED (Fig. 8b) [77]. This complex was taken up in the heart and to a smaller extent in the brain, but it had a high accumulation in the blood, and quickly washed out of the heart and brain.

2.3.5. ^{68}Ga-labeled brain imaging agents

The development of a Ga(III) agent that crosses the blood–brain barrier has been an elusive goal over the past 30 years. There are very few reports of radiogallium complexes that accumulate in the normal brain. The ^{68}Ga-labeled pyridinone derivatives developed by Zhang and coworkers showed uptake in rabbit brain that appeared to accumulate over several hours [74]. ^{68}Ga–THM_2BED showed slight uptake in the brain at very early times post-injection, but showed rapid washout [77].

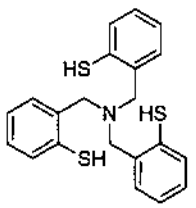

tris(2-mercaptobenzyl)amine (S_3N)

Fig. 8. (a) The N_2S_2 ligand BAT–TECH whose Ga(III) complex showed significant myocardial uptake in an animal model. (b) The hexacoordinate N_2O_4 ligand THM_2BED which showed both heart and brain uptake in rats.

More recently, Cutler and coworkers have shown that a small, neutral, lipophilic complex of ^{68}Ga labeled to a tris(2-mercaptobenzyl) amine (S_3N) ligand (Fig. 9) crosses the blood–brain barrier [78,79]. The ^{68}Ga–S_3N complex does not exhibit first-pass uptake into the brain (i.e. the highest uptake immediately after injection), but rather shows slower uptake in the brain followed by slow washout, with a brain:blood ratio of 3.5 at 15 min post-injection, increasing to 5.2 by 60 min. This agent exhibits the most promise for brain imaging of any ^{68}Ga complex evaluated to date.

2.4. Indium

2.4.1. Indium chemistry

The chemistry of indium is very similar to that of gallium. Both metals are only stable in the +3 oxidation state in aqueous solution. Many of the same nitrogen, oxygen and sulfur containing ligands bind both Ga(III) and In(III) with high stability. Gallium and indium are in group IIIB of the periodic table. Ga(III) is considered a hard metal ion, which prefers binding to hard oxygen donor ligands, whereas In(III) is considered intermediate with respect to the Hard Acid/Hard Base (HAHB) theory [80], preferring neutral nitrogen and negative sulfur donor atoms [81]. In(III) also hydrolyzes easily, forming insoluble hydroxides at pH > 3.4, and forms very strong complexes with transferrin [82].

2.4.2. Indium imaging agents

The most widely used radioisotope of indium for labeling radiopharmaceuticals is ^{111}In. ^{111}In ($T_{1/2} = 62$ h) is cyclotron produced, decays by electron capture (EC) with subsequent emission of gamma photons of 173 and 247 keV (89 and 94% abundance, respectively), and is widely used in gamma scintigraphy. ^{111}In was first evaluated in vivo in 1969 [83,84].

There have been a number of reviews which cover ^{111}In radiopharmaceuticals [85–89]. Many of the ^{111}In-labeled imaging agents that were developed in the 1970s are still used today. ^{111}In–DTPA has been used as a diagnostic agent for renal and brain imaging and is currently used for imaging flow changes and leakage of cerebrospinal fluid [90,91]. ^{111}In-labeled white blood cells (using ^{111}In–oxine) is an agent for imaging infection [92]. The majority of new ^{111}In radiopharmaceuticals are biomolecules such as proteins and peptides. These agents are discussed later on in Sections 2.8.2 and 2.8.4.

2.5. Ligands for forming stable Ga(III) and In(III) complexes

A large number of ligands have been designed for Ga(III) and In(III). In the design of metal complex radiopharmaceuticals, an important factor is thermodynamic stability. Thermodynamic stability does not necessarily indicate that the complex is stable in vivo; however, it is often used as a first criterion for designing radiopharmaceuticals. Table 3 lists the stability contants of Ga(III) and In(III) for polyaminopolycarboxylate, hydroxyaromatic, macrocyclic and amine–thiol type ligands.

Table 3
Stability constants of Ga(III) and In(III) complexes

Ligand	[ML]/[L][M]		pM		Ref.
	Ga(III)	In(III)	Ga(III)	In(III)	
Transferrin	19.8	18.3	19.7	18.3	[62,82]
EDTA	21.0	24.9	20.0	22.1	[93]
DTPA	24.3	29.0	20.2	24.9	[93]
PLED	32.3	26.5	24.7	19.0	[93,98]
HBPLED	31.0	29.0	21.8	19.7	[95]
DMPLED	27.3	21.5	25.5	19.7	[95]
Me_4HBPLED	31.9	33.0	24.6	20.6	[95]
HBED	38.5	28	28.7	20.0	[97]
THMBED	34.2	30.7	21.2	17.8	[99]
t-butyl-HBED	36.3	31.3	23.3	18.3	[99]
Me_4HBED	34.2	30.7	22.2	18.8	[99]
SHBED	37.4	29.4	27.2	19.2	[98]
HBMA	30.5	26.3	19.1	14.9	[99]
rac-TMPHPG	32.5	26.0	20.7	13.8	[101]
meso-TMPHPG	34.0	26.6	20.7	13.3	[101]
rac-EHPG	33.9	26.7	23.3	16.1	[100]
meso-EHPG	32.4	25.3	22.0	14.9	[100]
NOTA	30.1	26.2	26.4	21.6	[105]
DOTA	21.3	23.9	15.2	17.8	[106]
TETA	19.7	21.9	14.1	16.2	[106]
TACN–HB	40.5	33.3	23.4	16.6	[109]
TACN–TX	44.2	34.0	25.2	15.0	[345]
TACN–HP	42.0	25.08	32.1	15.2	[109]
TACN–meHP	45.6	28.02	34.9	17.4	[346,347]
TACN–TM	34.2	36.1	23.9	23.6	[108]
4SS	24.7	27.4	22.6	21.7	[118]
5SS	27.4	30.9	22.1	23.7	[118]
6SS	41.0	39.8	31.6	30.9	[118]
EDDASS	35.6	37.0	29.0	30.4	[118]
EC	31.5	33.0	NR	NR	[114,117]

2.5.1. Polyaminopolycarboxylate ligands

Although Ga(III) and In(III) are somewhat different with respect to their HAHB character, they both bind to polyaminopolycarboxylate ligands with high stability.

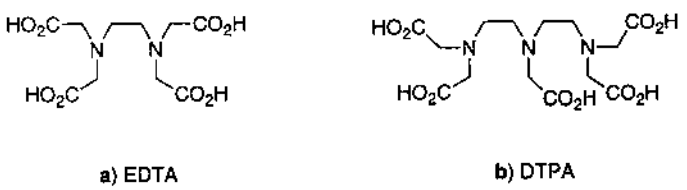

Fig. 10. The classic polyaminocarboxylate ligands EDTA and DTPA.

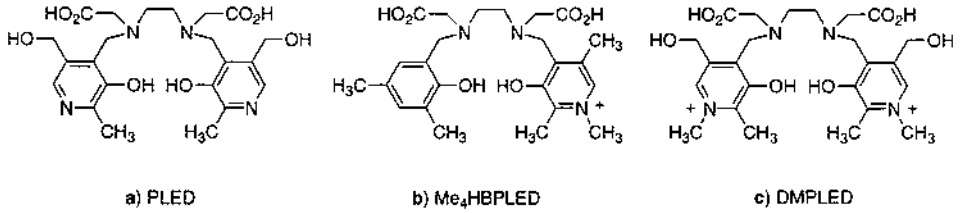

Fig. 11. Pyridoxylethylenediamine ligands for the complexation of Ga(III) and In(III).

The classic polyaminopolycarboxylate ligands EDTA and DTPA (Fig. 10) form strong complexes with Ga(III) and In(III), with the log stability constants in the range from 21 (for Ga–EDTA) to 29 (In–DTPA) [93]. Ga(III) and In(III) bind to EDTA and DTPA in a six-coordinate octahedral configuration.

2.5.2. Pyridoxylethylenediamine derivatives

In attempts to improve upon the chelates EDTA and DTPA and design more biologically stable Ga(III) and In(III) complexes for use as radiopharmaceuticals, the thermodynamic stabilities and in vivo behavior of a number of hexadentate ligands with an EDTA-type framework have been evaluated. The first type of agents investigated were *N*,*N*′-dipyridoxylethylenediamine-*N*,*N*′-diacetic acid (PLED) (Fig. 11a) [94], which form Ga(III) and In(III) complexes with a single negative charge. The Ga–PLED complex was more thermodynamically stable than either Ga–EDTA or Ga–DTPA; however, the In–PLED complex has showed intermediate stability that was greater than In–EDTA and less than In–DTPA [93]. Other derivatives were evaluated, including the addition of a methyl group to the pyridine nitrogen which increased the overall charge (Me_4HBPLED and DMPLED) (Fig. 11b and c). The In(III) complex of Me_4HBPLED with one hydroxybenzyl and one methylpyridoxyl moiety, had a thermodynamic stability >6 orders of magnitude higher than the parent In–PLED compound [95]. Conversely, the In(III) complex of DMPLED which has two methylpyridoxyl moieties, was 5 orders of magnitude less stable than the parent PLED compound. In normal rats, the PLED derivatives of ^{68}Ga and ^{111}In were cleared primarily through the kidneys and excreted into the urine [96]. Adding methyl substituents (DMPLED) increased the lipophilicity and somewhat increased the uptake in the liver; however, the clearance remained predominantly renal [96].

2.5.3. Hydroxyaromatic diamines

Another type of hydroxyaromatic ligand for Ga(III) and In(III) that was evaluated was *N*,*N*′-bis(2-hydroxy-3,5-dimethylbenzyl)ethylenediamine-*N*,*N*′-diacetic acid (HBED) (Fig. 12a). Ga–HBED was >14 orders of magnitude more stable than either Ga–EDTA or Ga–DTPA; however, the In–HBED complex was

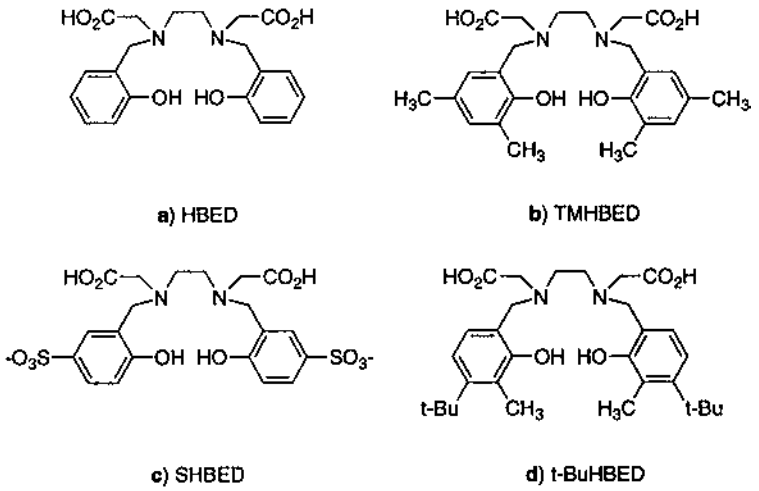

Fig. 12. Hydroxybenzylethylenediamine ligands for the complexation of Ga(III) and In(III).

10 orders of magnitude less stable than the Ga compound [97], and about one order of magnitude less stable than In–DTPA. Derivatizing HBED with various substituents on the phenyl ring (Fig. 12) decreased the stability of the Ga(III) complexes [95,98,99]. Adding methyl groups in the 2- and 4-position on the phenyl ring (TMHBED) and adding a sulfonyl group in the 4-position (SHBED) increased the stability of the In(III) complexes [99]. The addition of alkyl substituents ($TMMe_4HBED$, *t*-butyl HBED) significantly increased the amount of initial uptake of the ^{68}Ga and ^{111}In-labeled compounds in the liver in rats [96].

EHPG and its more lipophilic derivative TMPHPG (Fig. 13) [100,101] are derivatives of the previously discussed hydroxyaromatic ligands, but have carboxylate groups on the hydrocarbon backbone rather than the nitrogen. This derivatization gives rise to stereoisomers, and the racemic and meso forms of EHPG and TMPHPG have been separated and their stability constants measured. For both ligands (racemic and meso isomers), the Ga(III) complexes were >6 orders of magnitude more stable than the corresponding In(III)complex. The Ga(III) and In(III) racemic forms of the EHPG complexes were more stable than the meso

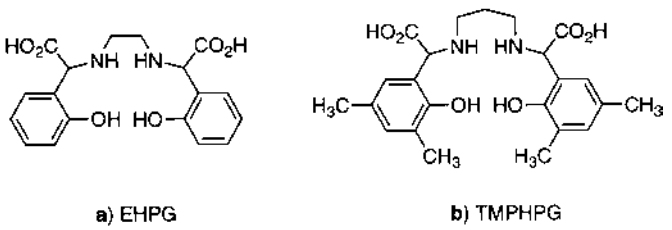

Fig. 13. Hydroxybenzylethylenediamine ligands with carboxylates located on the backbone instead of the amines. Both ligands possess steroisomers which are not indicated in the figure.

isomers, while for the TMPHPG the reverse was true. The in vivo results appeared to correlate with the thermodynamic stability; the ^{68}Ga-labeled EHPG and TMPHPG cleared rapidly out of the blood and liver and into the intestines, while the ^{111}In-labeled EHPG and TMPHPG did not clear from the blood as rapidly and the activity remained in the liver out to 2 h with no appreciable clearance [102,103]. The higher levels of blood and liver activity of the ^{111}In-labeled EHPG and TMPHPG suggest that the ^{111}In may have dissociated from the chelate and bound to serum and liver proteins.

2.5.4. Macrocyclic chelates

Another class of ligands for Ga(III) and In(III) that form very stable complexes of various charges are macrocyclic chelators. A variety of macrocycles containing nitrogen and oxygen or nitrogen and sulfur donor atoms have been evaluated. Three carboxylic acid derivatized macrocyclic chelators evaluated with Ga(III) and In(III) are NOTA, DOTA and TETA (Fig. 14). Craig and coworkers first published the crystal structure of Ga–NOTA [104]. This was followed by determination of the stability constant by Clarke and Martell [105]. The trends for the stability of the Ga(III) and In(III) complexes of the three ligands are the same for both metals: NOTA > DOTA > TETA [105,106]. The Ga(III) complex of NOTA is ca. 4 orders of magnitude greater than the In(III) complex; however, the In(III) complexes of DOTA and TETA are 2–3 orders of magnitude greater than Ga(III). The lower stability of In–NOTA versus Ga–NOTA could be due to the larger radius of the In(III) cation (94 pm) versus the Ga(III) cation (76 pm) and the smaller cavity size of NOTA. The higher selectivity of DOTA and TETA for In(III) is more likely due to steric factors [105].

The high stability of the Ga(III) and In(III) triazacyclononane (TACN) derivatives (Fig. 15) has led to the synthesis and evaluation of a number of other analogs. Moore and coworkers synthesized a thiol-derivatized TACN derivative (Fig. 15b) and published the crystal structure of the Ga(III) complex, showing the Ga(III) chelated in a slightly distorted octahedral environment [107]. The stability constants of Ga(III) and In(III) complexes of TACN–TM were considerably higher than the NOTA derivatives, with the In–TACN–TM having a stability 10 orders of magnitude higher than In–NOTA, demonstrating the greater affinity of In(III) for thiol containing ligands [108].

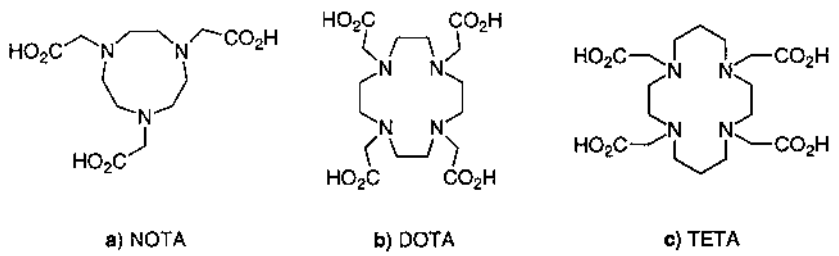

Fig. 14. Macrocyclic ligands which form stable complexes with both Ga(III) and In(III).

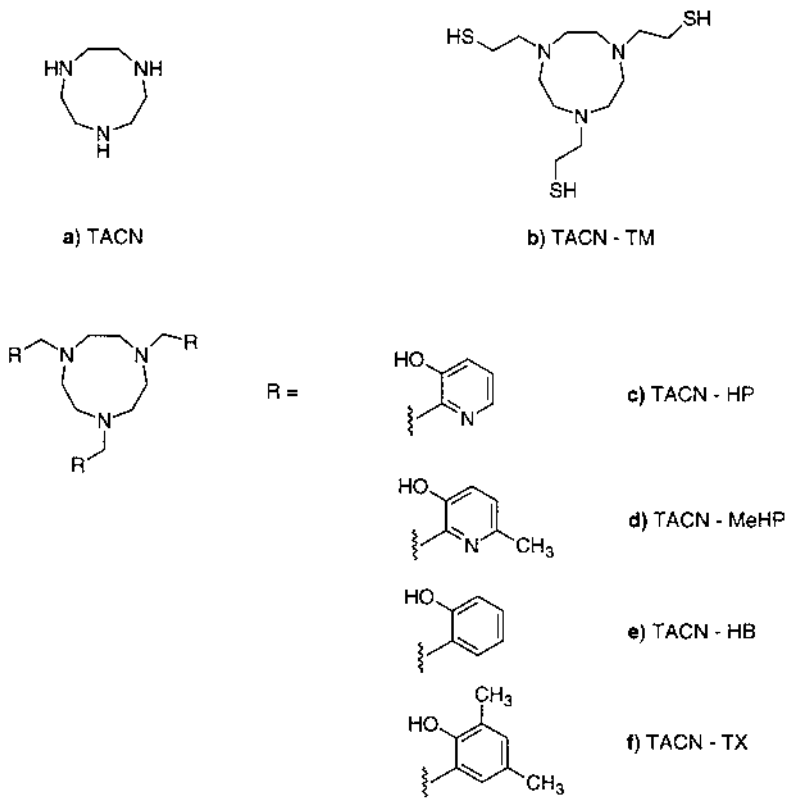

Fig. 15. Triazacyclononane and derivatives utilizied as Ga(III) and In(III) ligands.

Jones–Wilson and coworkers evaluated a number of different TACN derivatives (Fig. 15c–f) which contained either hydroxybenzyl or hydroxypyridyl groups on the nitrogens [109]. The stabilities of the neutral Ga(III) complexes were all more than 10 orders of magnitude higher than the Ga–NOTA complexes, indicating the high affinity of Ga(III) for the hydroxybenzyl and hydroxypyridyl moieties over an aliphatic carboxyl group. The more rigid structure of TACN ligands also may contribute to the greater stability. The Ga(III) hydroxypyridyl TACN derivatives were 17 orders of magnitude more stable than the In(III) derivatives, indicating the high selectivity of the hydroxypyridyl group for Ga(III) over In(III). The Ga(III) and In(III) hydroxypyridyl TACN complexes were much less stable under in vivo than the hydroxybenzyl derivatives.

2.5.5. Amino–thiol chelates

In more recent years, there have been efforts toward the development of a more stable chelate for In(III). This is due in part to the advent of ^{111}In-labeled mAbs and peptides using bifunctional chelating agents. Kung and coworkers evaluated four-coordinate N_2S_2 ligands (TE–BAT (Fig. 16b) and BAT–TECH (Fig. 8a)) for

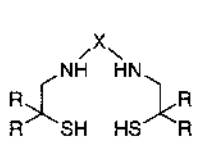

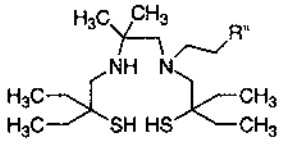

Compound	X	R	Compound	R"
a	CH_2CH_2	CH_3	f	diethylamine
b	CH_2CH_2	C_2H_5	g	pyrrolidine
c	$C(CH_3)_2CH_2$	CH_3	h	3-Methylpyrrolidine
d	$CH_2C(CH_3)_2CH_2$	CH_3	i	3,3'-Dimethylpyrrolidine
e	$CH_2C(CH_3)_2CH_2$	C_2H_5	j	3-Phenylpyrrolidine

Fig. 16. Aminothiol ligands for In(III). Compound b exhibited the highest myocardial uptake of the series.

In(III) and Ga(III) as potential myocardial imaging agents [75,110]. New synthetic methods to prepare macroscopic quantities of these Ga(III) complexes were published recently [111]. Cotsyfakis et al. reported the synthesis and mouse biodistribution results for a series of ten positively charged N_xS_2 complexes of In(III) (Fig. 16a–j) [112]. Of the ten aminothiol derivatives investigated, In–TE–BAT gave the highest heart:blood ratio.

John and coworkers carried out biodistributions in mice of two lipophilic ^{67}Ga agents: a thiol-derivatized TACN (Fig. 17a) and a ^{67}Ga-labeled N_3S_3 ligand (TMAE) (Fig. 17b) [113]. They found them to be stable in vivo, but the agents had no significant heart or brain uptake.

Hexacoordinate diamine dithiol dicarboxylate complexes have been found to form extremely stable complexes with In(III) [114–118]. In(III) and Ga(III) demonstrated log stabilities with *N,N'*-ethylene-di-l-cysteine (EC) (Fig. 18a) of 33.0 and 31.0, respectively [114,117]. A thiol containing derivative of EDTA was synthesized

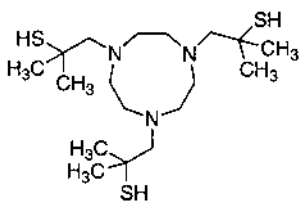

a

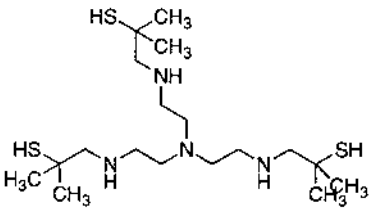

b

Fig. 17. Polyaminopolythiol ligands which complex Ga(III).

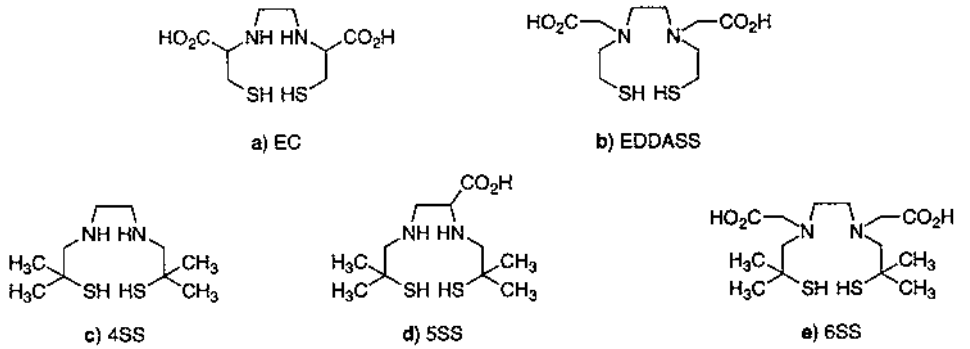

Fig. 18. A series of hexacoordinate N_2S_2 ligands for complexing Ga(III) and In(III). The In(III) complex of (**e**) has the highest stability of any In(III) complex reported to date.

by substituting two acetate groups for two mercaptoethyl groups (EDDASS) (Fig. 18b). The log stability of this ligand for In(III) was 37.0 [115]. The ligand that had the highest affinity for In(III) was a derivative of EDDASS that had geminal dimethyl groups on the carbon backbone (6SS) (Fig. 18e). The In–6SS complex had a log stability of 39.8 [118].

In the study by Sun et al., the thermodynamic stability of a series of 4, 5 and 6 coordinate $^{67/68}$Ga- and ^{111}In-labeled N_2S_2 complexes (4SS, 5SS, 6SS, and EDDASS) (Fig. 18b–e) was correlated with in vivo behavior [118]. The 6-coordinate complexes also had a >9-fold increase in stability over the four- and five-coordinate complexes. The six-coordinate complexes cleared more rapidly through the liver than the four- and five-coordinate complexes. Similar behavior was observed for ^{67}Ga- and ^{111}In-labeled EC [114], where the more stable ^{111}In–EC cleared more rapidly than ^{67}Ga–EC. Although no experiments were carried out to verify the fate of the radiolabel in the liver, the more rapid clearance of the 6-coordinate complexes was likely due to the complexes being excreted intact, whereas retention in the liver of the four- and five-coordinate complexes may have been due to the radiometal becoming dissociated from the chelate with subsequent binding to proteins.

2.6. Copper

The radionuclides of copper offer a selection of diagnostic (^{60}Cu, ^{61}Cu, ^{62}Cu and ^{64}Cu) and therapeutic (^{64}Cu and ^{67}Cu) isotopes (Tables 1 and 2). The positron-emitting diagnostic isotopes have a wide range of half lives (10 min to 12.7 h) and are cyclotron or generator produced. The improved production of copper isotopes is currently under investigation and the efficient production of high purity and high specific activity ^{60}Cu, ^{61}Cu and ^{64}Cu by a biomedical cyclotron has been reported recently [119,120]. All aspects of copper radionuclide production, chemistry, radiochemistry and radiopharmacology have been published in an exhaustive review by Blower et al. in 1996 [121].

The use of copper radionuclides presents many advantages over those of the established radionuclides such as ^{99m}Tc. The chemistry of copper is restricted to two principle oxidation states (I and II) and the relatively simple coordination and redox chemistry of copper is well documented. Copper is ubiquitous in nature and its biochemistry and metabolism in humans is well known. The physical properties of the available isotopes have lead to the development of kinetically inert copper complexes for long term targeting and trapping (e.g. radiolabeled antibodies), and those selectively trapped in tissues by redox-catalyzed ligand exchange mechanisms (e.g. blood flow tracers). We will discuss some new developments in the area of copper radiopharmaceuticals since the publication of the 1996 review.

2.6.1. Metabolism of copper chelates

The choice of bifunctional chelate moiety is highly dependent on the stability it confers to the metal center. Motekaitis and co-workers measured the stability constants of two macrocyclic chelates and their corresponding bifunctional chelates (Fig. 19) [122]. They determined that adding a functional group to one of the nitrogens on either cyclam (1,4,8,11-tetraazacyclotetradecane) or 15aneN5 (1,4,7,10,13-pentaazacyclopentadecane) decreases the stability about 2–4 orders of magnitude, with the functionalized cyclam derivative showing the greater decrease in stability.

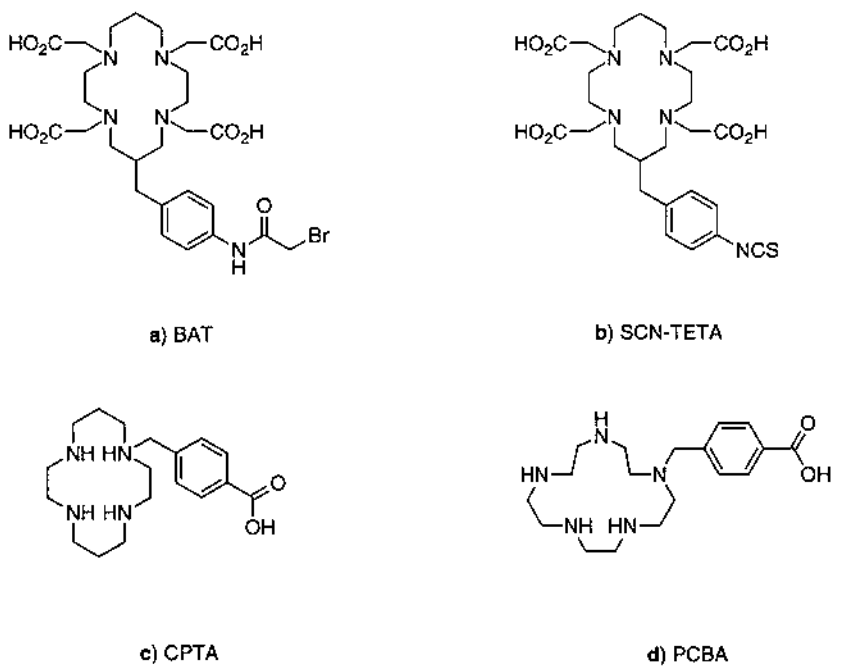

Fig. 19. Macrocyclic bifunctional chelates for Cu(II).

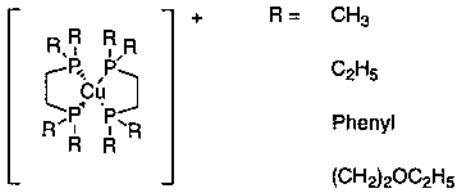

Fig. 20. Bis(diphosphine) ligands for complexing Cu(I).

The choice of chelate can dramatically affect the biokinetics, distribution and metabolism of the radiopharmaceutical which will ultimately determine the clinical usefulness of the drug. A recent study on four copper chelates has shown that chelate charge and lipophilicity play a role in kidney retention of copper radiolabeled antibodies and that transchelation of the copper radiolabel appears to be a significant factor for accumulation in the liver [123].

2.6.2. MDR imaging agents

As discussed with ^{99m}Tc agents (Section 2.1.1), lipophilic cations can act as substrates for Pgp and therefore be useful in the detection of MDR in tumors. In 1996, a series of ^{64}Cu(I)–bis(diphosphine) complexes (Fig. 20) were evaluated in vitro and in vivo [124]. These lipophilic, stable complexes are easily and efficiently produced. The complexes are tetrahedral and cationic and act as substrates for Pgp in vitro [125].

2.6.3. Hypoxia imaging agents

The use of redox active compounds for the detecting tissue ischemia was described in Section 2.1.2. Fujibayashi and coworkers have shown that the bis(thiosemicarbazone) complex, Cu(II)–diacetyl-bis(N^4-methylthiosemicarbazone) (^{62}Cu–ATSM) (Fig. 21a), is trapped selectively in hypoxic tissue [126]. The copper(II), neutral, square–planar complex exhibits high membrane permeability and low redox potential. The analogous complex, Cu(II)–pyruvaldehyde-bis(N^4-methylthiosemicarbazone) (Cu–PTSM) (Fig. 21b), is a proven blood flow tracer that becomes trapped in most major tissues (e.g. brain, heart, liver, kidney) and even tumors [121]. More recently it has been shown to be trapped in rat brains after

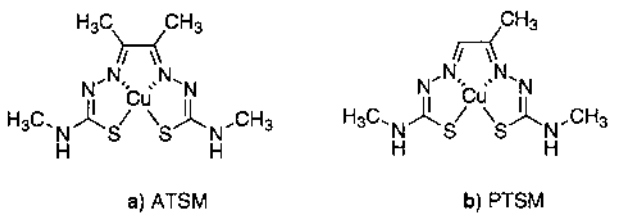

Fig. 21. Bis(thiosemicarbazone) Cu(II) complexes utilized for imaging hypoxic tissue (**a**) and for perfusion (**b**).

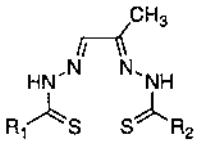

a	$R_1 = NHCH_3$	$R_2 = NH_2$
b	$R_1 = NH_2$	$R_2 = NHCH_3$
c	$R_1 = N(CH_3)_2$	$R_2 = NH_2$
d	$R_1 = N(CH_3)_2$	$R_2 = NHCH_3$

Fig. 22. Mixed bis(thiosemicarbazone) ligands for complexing Cu(II).

transient global ischemia [127]. By the simple addition of the methyl group to PTSM (pyruvaldehyde to diacetyl) the redox potential of the complex was altered. Cu(ATSM) has a lower redox potential (-297 mV) compared to that of Cu(PTSM) (-208 mV). This difference in the redox values was postulated to be the primary reason for the selective trapping of Cu(ATSM) in highly reductive hypoxic tissue, but not in less reducing normal tissue.

Although not presented as possible hypoxia agents, a 1997 report describes new mixed bis(thiosemicarbazone) ligands (Fig. 22) as possible new radiopharmaceuticals [128]. The ^{62}Cu complexes of these tetradentate thiosemicarbazone ligands were produced and evaluated in rat models. The approach of using dissimilar thiosemicarbazone moieties may dramatically effect the redox properties of the complexes and as a consequence produce cerebral and myocardial agents and aid in the detection of ischemia.

2.7. Yttrium

A review on the general coordination chemistry of yttrium has been presented [129] which focuses on novel compounds that have been structurally characterized, but does not focus on compounds of biological interest. Here, we will describe briefly some complexes of yttrium that are of interest in medicine.

There are two radioisotopes of yttrium that have been utilized in preparing radiopharmaceuticals: ^{90}Y ($T_{1/2} = 64.06$ h) and ^{86}Y ($T_{1/2} = 14.7$ h). Yttrium-90 is a pure β^- emitter, and therefore has applications for targeted radiotherapy. Yttrium-86 is a positron-emitter, and has been used as an alternate label for ^{90}Y for applications in PET imaging [130–132].

In aqueous solution, the most prevalent species present is Y(III), and therefore, many of the same chelates that complex In(III) in a stable configuration have been utilized with Y(III). The majority of studies using yttrium radioisotopes involve the labeling of ^{90}Y or ^{86}Y to larger biomolecules through bifunctional chelates (see Section 2.8.1), generally, derivatives of DTPA and DOTA. It has been shown that in vivo ^{90}Y dissociates from DTPA and accumulates in the bone [133]. For this reason, the macrocyclic chelate DOTA has replaced DTPA since it forms more kinetically stable complexes [134]. Further discussion on ^{90}Y and ^{86}Y-labeled biomolecules will be presented in Section 2.8.2.1.

2.8. Radiometal-labeled biomolecules

2.8.1. Bifunctional chelates and direct methods of labeling

Within the last 10 years, there has been a considerable amount of research in the area of radiometal-labeled receptor targeted agents. Receptor ligands can be larger biomolecules such as peptides, or smaller organic molecules such as dopamine or folic acid. The radiometal is connected to these biomolecules via a bifunctional chelating agent (BFC), which consists of a chelate to complex the radiometal and a functional group for attachment to the biomolecule. Functional groups that form amide, thiourea, urea, Schiff-base, or thioether linkages with amine or thiol groups on proteins and peptides have been described [8,135–141]. The first BFCs described were analogs of EDTA and DTPA [142–145]. Several improvements have been made to the originally developed BFCs, and they are described in a review article by Gansow [140]. Commonly used BFCs for radionuclides of copper, technetium, and rhenium are described in a review article by Schubiger et al. [141]. Two other thorough reviews by Jurisson et al. and Hnatowich describe BFCs designed for isotopes of indium, technetium, yttrium, and rhenium [3,146]. Eckelman has published an exhaustive review of ^{99m}Tc radiopharmaceuticals that includes a fairly complete section on BFCs for labeling peptides and proteins with ^{99m}Tc [7].

Alternative methods for labeling proteins and peptides with ^{99m}Tc involve reducing intramolecular disulfide bonds to generate thiol groups which have high affinity for Tc(V). Several review articles discuss the various direct labeling methods for ^{99m}Tc and rhenium isotopes and proteins [146–149]. More recently, methods for direct labeling of ^{99m}Tc- and ^{188}Re-peptides have been reported [150–152]. We will discuss radiometal biomolecule conjugates by the type of diseased tissue they target.

2.8.2. Tumor targeting agents

The radiolabeling of antibodies for the detection of cancer in the early 1970s [153–155] marked the beginning of the use of radiolabeled proteins and peptides for targeting antigens and receptors that are upregulated in tumors. Initially, radiolabeled antibodies were labeled with iodine radionuclides, but currently, the use of radiometal-BFC-antibody conjugates is becoming more prevalent. Over the last 25 years, the field of radioimmunoscintigraphy (RIS) and radioimmunotherapy (RIT) has grown such that there are currently three RIS agents approved for clinical use in the USA (Section 2.8.2.3). More recently, since the early 1980s, the radiolabeling of receptor ligands for cancer imaging has become very widespread, and there is one radiometal-labeled receptor agent approved for use in the USA (Section 2.8.2.1). This section of the review will focus on radiometal-labeled receptor ligands for oncological imaging.

2.8.2.1. Somatostatin analogs. Some of the first peptide-based tumor receptor imaging agents were radiolabeled analogs of the hormone somatostatin. Somatostatin is a 14-amino-acid peptide involved in the regulation and release of a number of hormones, including growth hormone, thyroid-stimulating hormone and prolactin. Somatostatin receptors (SSR) occur in a number of different normal organ

systems such as the central nervous system, the gastrointestinal tract, and the exocrine and endocrine pancreas [156–158]. A large number of human tumors are also somatostatin receptor-positive [159]. Somatostatin has a very short biological half-life and analogs have been developed, such as octreotide, which show much longer residence times [160]. Octreotide, an 8-amino acid SS analog, has been labeled with ^{111}In using a BFC of DTPA [161,162], (Fig. 23), and is approved for human use in the USA and Europe as a diagnostic imaging agent for neuroen-

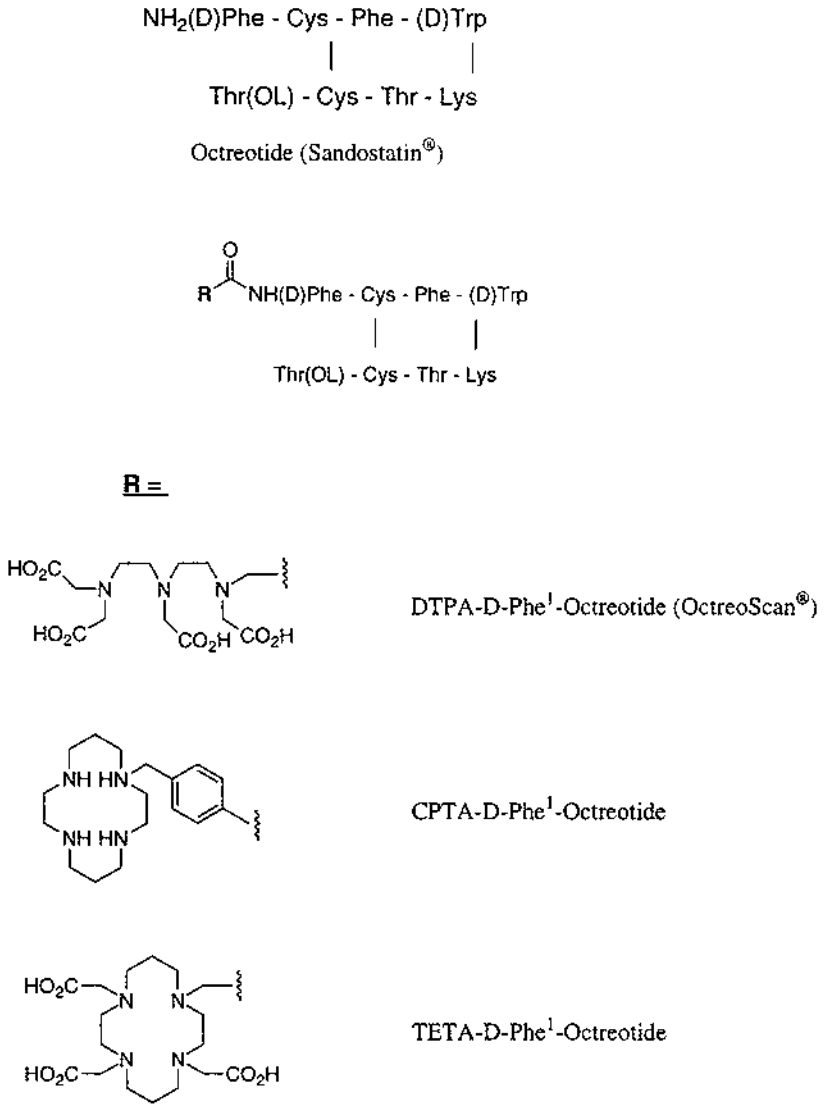

Fig. 23. The somatostatin analog octreotide and BFC-octreotide conjugates for radiometal labeling.

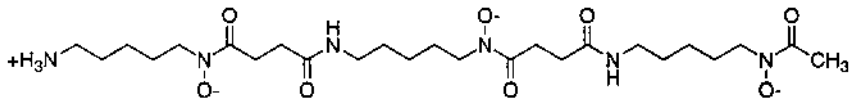

Fig. 24. of the ligand desferrioxamine-B.

docrine tumors [163]. Somatostatin analogs, including octreotide, RC-160, and several developed by Diatide, have been labeled with a wide variety of metal radionuclides, including ^{64}Cu, ^{68}Ga, ^{99m}Tc, ^{188}Re and ^{90}Y, for diagnostic imaging and radiotherapy. In the following section, several of these will be discussed.

^{68}Ga–DTPA–octreotide was prepared, but dissociation of the ^{68}Ga occurred upon incubation in serum [164]. A BFC of HBED was also conjugated to octreotide; this agent was not investigated in vivo due to the hydrophobic and insoluble nature of the HBED–octreotide conjugate [164]. ^{68}Ga and ^{67}Ga have been labeled to octreotide using the BFC desferrioxamine-B (DFO) (Fig. 24) [164,165]. DFO, a well-known chelate with high affinity for Fe(III), is used for treating iron overload [166,167] and forms a stable, neutral complex with Ga(III) by coordination through three hydroxamate groups. DFO has an amino group of relatively high reactivity that allows conjugation to peptides or proteins, and it has been conjugated to HSA [168]. $^{67/68}$Ga–DFO–octreotide was stable in vivo and showed high affinity for the SSR both in vitro and in vivo. The biological clearance of $^{67/68}$Ga–DFO–octreotide was rapid, and the conjugate was excreted through the kidneys and into the urine, similar to ^{111}In–DTPA–octreotide. This agent has potential as a PET agent for imaging SSR positive tumors.

Octreotide has been conjugated to two macrocyclic bifunctional chelates, CPTA and TETA (Fig. 19c and Fig. 14c), for labeling with ^{64}Cu [169]. Because of the lability of copper, macrocyclic chelates are necessary to form complexes that are stable in vivo. CPTA, a derivative of cyclam, forms Cu(II) complexes having a $+1$ charge, whereas the Cu–TETA complex has a -1 charge. ^{64}Cu–CPTA–octreotide and ^{64}Cu–TETA–octreotide (Fig. 23) had high affinity for the SSR both in vitro and in vivo, but the biological clearance was very different between the two conjugates. The ^{64}Cu–CPTA conjugate cleared almost exclusively through the liver, and the clearance was very slow. This contrasted dramatically with ^{64}Cu–TETA–octreotide, which cleared primarily through the kidneys, with very low liver accumulation. These results demonstrate that the BFC has a major impact on the biological behavior of radiometal-BFC-biomolecule conjugates. ^{64}Cu–TETA–octreotide is currently being evaluated as a PET imaging agent for neuroendocrine tumors [170]. Preliminary results showed that ^{64}Cu–TETA–octreotide was able to detect even more SSR positive lesions than the currently used agent, ^{111}In–DTPA–octreotide and gamma scintigraphy.

Octreotide analogs have also been labeled with ^{86}Y (PET imaging) and ^{90}Y (radiotherapy) through DTPA and DOTA chelates [131,132,171–173]. The DTPA chelate was shown to be a suboptimal chelate for ^{90}Y due to the in vivo instability

of ^{90}Y–DTPA, resulting in high bone uptake [131,171]. ^{90}Y–DOTA was found to be very stable in vivo, and $^{86/90}$Y–DOTA–Tyr^3–octreotide demonstrated high target uptake and rapid renal clearance [132,172]. Clinical trials for PET imaging and radiotherapy using ^{86}Y- and ^{90}Y-labeled DOTA–Tyr^3–octreotide are imminent [132,172].

^{99m}Tc has been conjugated to the somatostatin analog RC-160 using bifunctional chelates such as CPTA and HYNIC, and also by direct labeling methods, where the ^{99m}Tc was complexed to free thiols generated by reduction of the disulfide bond in octreotide [152,174]. In these preparations, reducing agents for the disulfide bond as well as the $^{99m}TcO_4^-$ were included in the reaction. The pertechnetate (^{99m}Tc(VII)) was reduced to ^{99m}Tc(V) with $Na_2S_2O_4$ while the reducing agent for octreotide's disulfide bond was ascorbic acid [151]. The biodistributions of directly labeled ^{99m}Tc–RC-160 and ^{99m}Tc–CPTA–RC-160 in tumor-bearing mice demonstrated similar uptake in both target and non-target organs [152]. Zamora et al. have labeled RC-160 with ^{188}Re using a direct labeling method where stannous ions serve the dual purpose of reducing both perrhenate and the disulfide bond in the peptide [175,176].

Technetium and rhenium have been complexed to somatostatin analogs via chelates formed from peptides containing the amino acids glycine, cysteine and lysine [177]. These chelators included bisamide bisthiols, provided by the sequence –Cys–Gly–Cys–, triamide thiols provided by the sequence –Gly–Gly–Cys– and a diamide–amine–thiol of the type –(ε-Lys)–Gly–Cys and bound oxo–rhenium(V) and oxo–technetium(V) in a tetradentate fashion (Fig. 25). Using small

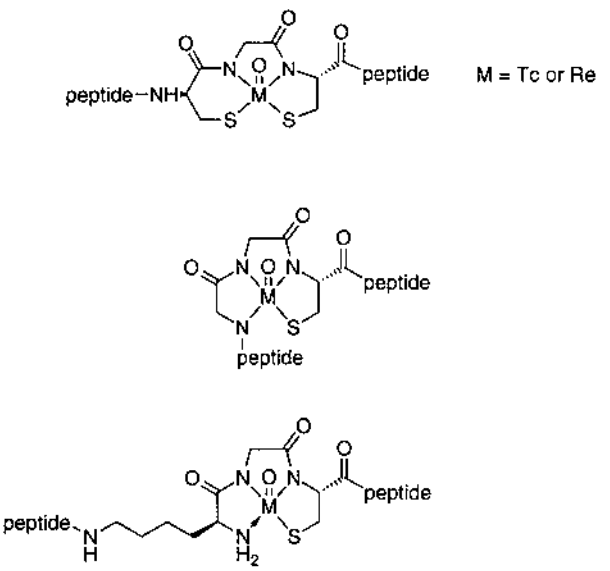

Fig. 25. Peptide based ligands for Tc and Re which can then be conjugated to peptide-receptor ligands.

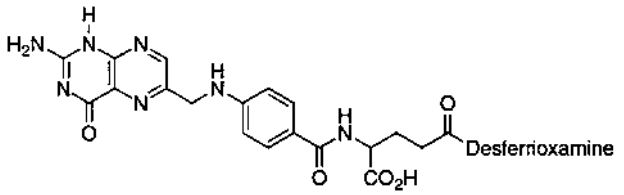

Fig. 26. The folate-DFO bioconjugate which has been labeled with ^{67}Ga.

peptides as chelators for peptide receptor ligands greatly simplifies the synthesis of these chelate-receptor ligand bioconjugates. Two of the peptides evaluated in vitro by Pearson et al., ^{99m}Tc-labeled P587 and P829 [177], were studied further in animal models [178]. These ^{99m}Tc-labeled peptides were both found to have high binding affinity to the SSR in tumor-bearing rats and had clearance characteristics favorable for further clinical investigations, which are currently ongoing [179].

2.8.2.2. Folate receptor ligands. The chelate DFO was used to chelate Ga(III) to the vitamin folic acid (Fig. 26) [180]. A mixture of two isomers, DFO–folate (α) and DFO–folate (γ), was formed, since DFO was conjugated to two different carboxyl groups on folate. The γ isomer is the only one recognized by the folate receptor. ^{67}Ga–DFO–folate (γ) showed specific binding to the folate receptor, both in vitro and in vivo in a tumor-bearing mouse model [181]. DTPA has been conjugated to folate and labeled with ^{99m}Tc and ^{111}In [182,183].

2.8.2.3. Radiolabeled mAbs. Monoclonal antibodies (mAbs) have been produced which bind to antigens present on a large number of tumor types. mAbs have been labeled with radiometals for diagnosis and therapy of cancer, and this has been a subject in many reviews published in the last 10 years [7,141,184–192]. Intact mAbs are large proteins with a M_w of 160 kDa, and because of their large size, they have very slow biological clearance and are excreted through the hepatobiliary system. To circumvent these drawbacks, mAb fragments have been produced that have molecular weights ranging from 10–100 kDa. Metal radionuclides that have been labeled to mAbs (both intact and fragments) for diagnostic imaging include ^{111}In, ^{67}Ga, ^{99m}Tc and ^{64}Cu. Currently, three mAb agents, ^{111}In–DTPA-B72.3 (OncoScint™), ^{111}In–DTPA-7E11.C5.3 (ProctaScint™) and a ^{99m}Tc direct-labeled Fab fragment of IMMU-4 (CEA–SCAN™) are approved for clinical use in the USA

2.8.2.4. Steroid receptor ligands. During the early 1980s, steroid ligands were labeled with radiohalogens and evaluated as imaging agents for hormone receptor-positive tumors [193–195]. Because of the favorable properties of ^{99m}Tc for nuclear medicine imaging, recent efforts have been made to develop a ^{99m}Tc-labeled steroid for imaging receptor-positive breast cancer (Fig. 27a). Dizio et al. were the first researchers to synthesize BFC–progestin conjugates, label them with ^{186}Re and ^{99m}Tc and evaluate them in vitro and in vivo for binding to the progestin receptor

[196,197]. The BFC utilized was a bisaminethiol (BAT) with geminol dimethyl groups on the carbon backbone. The ^{99}Tc and Re complexes of the BAT–progestin conjugates had affinity to the progestin receptor that was higher than progesterone itself, and there was specific uptake by the progestin receptors in the immature rat uterus; however, the lipophilicity of the conjugates (log partition coefficient of 6.4) caused high uptake in non-target organs such as the liver, fat and muscle [197].

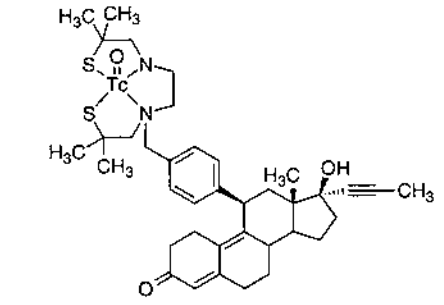

a

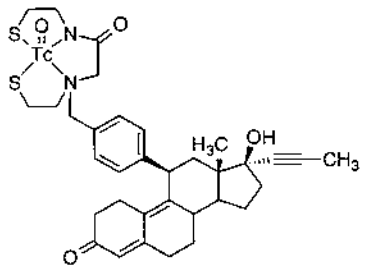

b

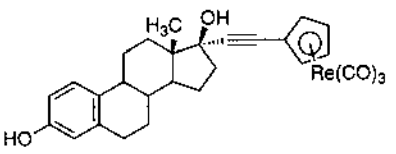

c

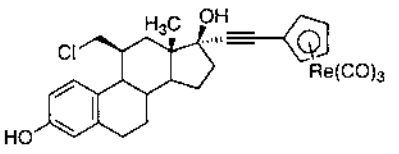

d

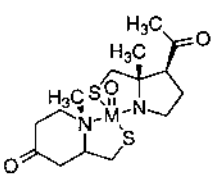

e

Fig. 27. Steroid based bioconjugates. Compounds (**a**) and (**b**) are N_2S_2–progestin conjugates for labeling with Tc and Re isotopes. Compounds (**c**) and (**d**) are organometallic–estrogen analogs. Compound (**d**) integrates the Tc or Re monooxo cation into the steroid structure.

O'Neil and coworkers made a less lipophilic agent consisting of a progestin–monoamine–monomide (MAMA′) bisthiol conjugate (Fig. 27b) [198]. This ^{99m}Tc agent was an order of magnitude less lipophilic (log partition coefficient of 4.9–5.25) and demonstrated a somewhat higher binding to the progestin receptor in vitro in rat uterine cytosol (0.965 vs 2.74 nM for ^{99m}Tc–BAT–progestin); however, the non-target uptake remained high.

Another approach to conjugating a metal complex to a steroid was described by Top and coworkers [199]. They prepared a series of (cyclopentadienyl)$Re(CO)_3$ conjugates of estradiol (Fig. 27c and d), where the organorhenium fragment is stably bonded at the 17α position. These compounds had high binding affinity for the estrogen receptor, and one of the derivatives (with a 11β-chloromethyl substituent) had an affinity higher than estradiol itself. The lipophilicities of these agents were high (log partition coefficients > 5), and as of this writing, no in vivo results have been reported.

Katzenellenbogen and coworkers have formulated an alternative method for preparing radiometal-steroid conjugates which involves integrating the radiometal within the steroid structure rather than attaching a separate chelate off the steroid backbone (Fig. 27e). The first model compounds of the metal-integrated steroid complexes were constructed as heterodimers from two different amino thiols [200,201]. These agents were labeled with ^{99m}Tc and shown to have in vivo stability comparable with ^{18}F-labeled steroids. In subsequent studies, Hom et al. prepared a series of bis-bidentate complexes of Re(V) that mimic the size, shape and peripheral functionality of steroidal androgens [202]. Although these complexes provided an impressive structural and stereochemical mimic of a steroid, the stability of the complex was less than optimal, with significant decomposition occurring in buffer over a period of less than 2 h. Probably for this reason, the in vitro receptor binding studies showed very low affinity for the androgen receptor.

Although a ^{99m}Tc-labeled steroid receptor ligand with optimal in vivo properties has not yet been realized, significant advances have been made over a relatively short period of time. Considering the high percentage of the population afflicted with either breast or prostate cancer, the pursuit of an effective diagnostic agent to aid in the determination of the receptor status of these cancers is a worthwhile goal.

2.8.2.5. Other tumor-receptor ligands. Sigma receptors have been shown to be expressed in a number of human tumor cells. John and coworkers have conjugated a bisaminothiol (BAT) chelate to *N*-methyl-2-piperidinylethyl amine (EN6) [203]. Scatchard analysis demonstrated specific binding of the ^{99m}Tc–BAT–EN6 conjugate to T47D breast cancer cells and biodistribution data in normal rats showed uptake in normal organs known to contain sigma receptors that was blocked upon co-injection of a sigma receptor ligand.

Giblin and coworkers demonstrated that the peptide *N*-acetyl–Cys–Gly–Cys–Gly forms a very stable complex with Re(V)–oxo core, and when complexed to the N termini of α-melanocyte stimulating hormone (α-MSH), the bioconjugate maintains the bioactivity of the native peptide [204]. This method of complexing Re(V) and Tc(V) is greatly simplified over the conjugation of a bifunctional chelate, and

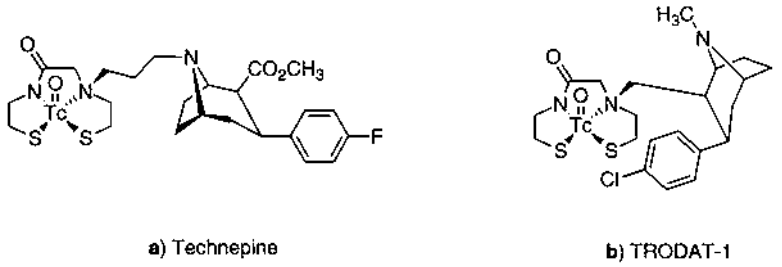

Fig. 28. Technetium labeled tropane derivatives for imaging dopamine transporters.

may have wide-spread applicability for labeling technetium and rhenium radionuclides to other peptides.

2.8.3. Neuroreceptor ligands

The imaging of dopamine transporters (DATs) with ^{99m}Tc may lead to significant advances in the detection and treatment of brain disorders such as Parkinson's and Alzheimer's diseases. DATs are located on dopamine neurons (presynaptically at dopaminergic nerve terminals) and a depletion in DAT levels is noted in sufferers of the above diseases with a concomitant loss of dopamine [205].

The development of ^{99m}Tc agents to target this indicator of neuronal loss has involved considerable effort. Specific chemical and biological restraints hinder the development of suitable agents due to the selectivity of DAT and other transporter systems. The metal chelate employed must not affect receptor binding and in vivo kinetics, it must further produce a neutral charge when complexed to the metal, permeate the lipid bilayer and cross the blood-brain barrier.

The first agent that was reported as a transport mediated ^{99m}Tc-based in vivo SPECT imaging agent (in primates) was Technepine (Fig. 28a) [206]. The compound has been shown to target and label the DAT receptors in the primate brain [207], selectively accumulating in striatum versus cerebellum (2:1 in the female monkey, 3:1 in the male monkey). Although previous agents had bound with high affinity to DATs, uptake was insufficient to obtain SPECT images in primates [208,209].

Technepine contains a highly selective and potent tropane for DAT receptor binding and a chelating agent that firmly complexes technetium. These two parts of the molecule are connected by a propyl linking group. The reduction of $^{99m}TcO_4^-$ in the presence of stannous ion and the soft ligand donor sets N_2S_2 and NS_3 produce Tc complexes of the form $(Tc^VO)^{3+}N_2S_2$ and $(Tc^VO)^{3+}NS_3$. The use of an N_2S_2 binding moiety conveys lipophilicity and a square pyramidal geometry to the technetium(V) metal center [210–212] and has been used in the labeling of biomolecules with ^{99m}Tc [198,213]. Formation of $(TcO)^{3+}$ complexes with mono-*N*-substituted N_2S_2 ligands can produce up to four isomers and Technepine is a 1:1 diastereomeric mixture. Attaching the bulky chelator to the 8-amino position of the tropane backbone does not adversely affect the binding ability of the tropane to the dopamine receptor.

A similar compound, [^{99m}Tc]TRODAT-1 (Fig. 28b), also contains the $(Tc^{V}O)^{3+}$ N_2S_2 core and has selectivity for dopamine transporters in the striatum region of the brain in rats and a baboon [214]. The chelator was attached to the tropane moiety in the 2β-position, compared to the 8-amino position, in an attempt to reduce the molecular weight of the final compound and to improve initial brain uptake. A report of this compound in humans further supports the use of this compound in the detection and imaging of DATs [215].

2.8.4. Agents for imaging infection

The identification of infection and inflammation in patients is the first step in the successful clinical management of infected sites. The first report of a diagnostically useful radiolabeled chemotactic peptide was in 1991 by Fischman and co-authors [216]. Chemotactic analogs of the peptide *N*-formyl-methionyl-leucyl-phenylalanine (ForMLF), a bacterial product, were labeled with ^{111}In using DTPA as the bifunctional chelate. Chemotactic peptides labeled with ^{99m}Tc via the hydrazinonicotimamide moiety (HYNIC) [217] can localize in infected areas [6,218–221]. The binding of HYNIC to ^{99m}Tc is not fully understood. The Tc(V) core, of possible

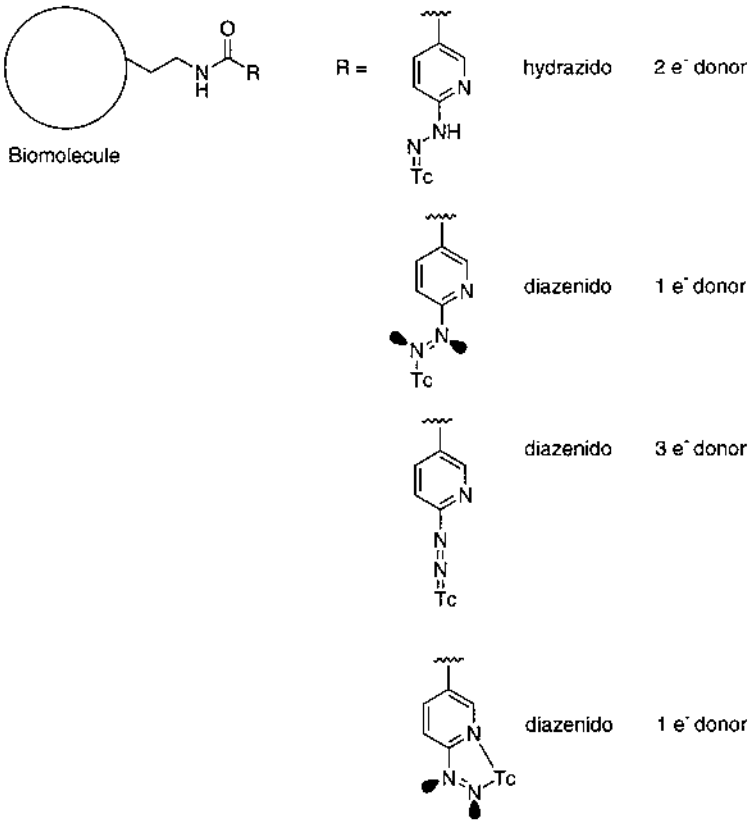

Fig. 29. Possible Tc binding modes of the HYNIC ligand.

distorted octahedral geometry, is bound to the HYNIC ligand presumably through a hydrazido or diazenido linkage (Fig. 29). The HYNIC ligand only occupies two sites of the Tc-coordination sphere; therefore, the co-ligand which fulfills the Tc metal ions coordination requirements is very important. The biokinetics of ^{99m}Tc–HYNIC-peptide depends on whether mannitol, tricine, glucarate, glucamine or glucoheptonate is used as the co-ligand [222,223]. The peptide *N*-formyl-methionyl-leucyl-phenylalanine-lysine (fMLFK), conjugated to HYNIC and labeled with ^{99m}Tc, was shown in two complementary reports to specifically localize at the site of infectious foci in rabbit [223,224]. There is a discrepancy on whether ^{99m}Tc–HYNIC–fMLFK can distinguish between infection and inflammation [221,223] and a recent editorial review [225] has compared and contrasted all aspects of ^{99m}Tc–fMLFK to provide a rational view for the possible use of this imaging agent.

2.8.5. Thrombus imaging agents

The early detection and localization of thrombi in patients is of paramount importance to the medical community as thrombus formation after surgery can seriously complicate the successful treatment of a patient. A non-invasive, fast method of thrombus detection is required and the use of a radiopharmaceutical is ideal for this purpose [226]. Many efforts have been made in the ^{99m}Tc-labeling of antibodies and some peptides to target thrombus, but have suffered largely from slow kinetics, unsuitable production methods or loss in binding affinity [227–229]. New synthetic peptides and antibody fragments labeled with ^{99m}Tc have improved recently clinical utility [230–236].

A N_3S bifunctional chelating system has been employed to produce the platelet receptor-binding imaging agent ^{99m}Tc–P748, which exhibits high receptor-binding affinity for venous thromboembolism [236,237]. The authors used a dimeric peptide, specific to the platelet GPIIb/IIIa receptor and a novel ^{99m}Tc binding chelate (Fig. 30). The 26 amino-acid peptide P280, specific to the same platelet receptor, has been investigated clinically and is a safe and sensitive marker for diagnosing pulmonary deep venous thromosis and pulmonary embolism [234]. Its pharmacokinetics are faster than that of ^{99m}Tc–P748 but it has a lower binding affinity for the GPIIb/IIIa receptor [227].

^{99m}Tc has been conjugated to cyclic GPIIb/IIIa receptor antagonists as well. The cyclic peptides have been labeled with ^{99m}Tc using donor sets such as N_2S_2 diaminethiols, an N_2S_2 monoamide–monoaminithiol, and N_3S triamidethiols (Fig. 31) [238–241]. These researchers have also used the HYNIC conjugation system

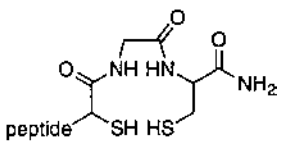

Fig. 30. A novel N_2S_2 Tc binding ligand which is conjugated to a peptide serving as a substrate to the platelet GPIIb/IIIa receptor.

with the GPIIb/IIIa receptor to produce cyclo(d-Val–NMeArg–Gly–Asp–Mamb(5-(6-(6-hydrazinonicotinamido)-hexanamide))) (HYNICtide) [242–244]. Due to the Tc-coordination requirements with HYNIC as discussed in the earlier section, tricine was used as a co-ligand, forming the complex [^{99m}Tc(HYNICtide)(tricine)$_2$] [242]. This compound was found to exist in a number of isomeric forms. Although initial biological data was promising [243], the complex was unsuitable for clinical use due to instability in aqueous solution, a possible consequence of the isomerism of the tricine and the HYNIC moiety [239]. In order to minimize the isomeric and solution stability problems, aminocarboxylate derivatives were employed as co-ligands, improving solution stability but retaining three isomeric forms [242]. An alternative approach used water soluble monophosphines as the co-ligands. Synthetic pathways were readily available and a

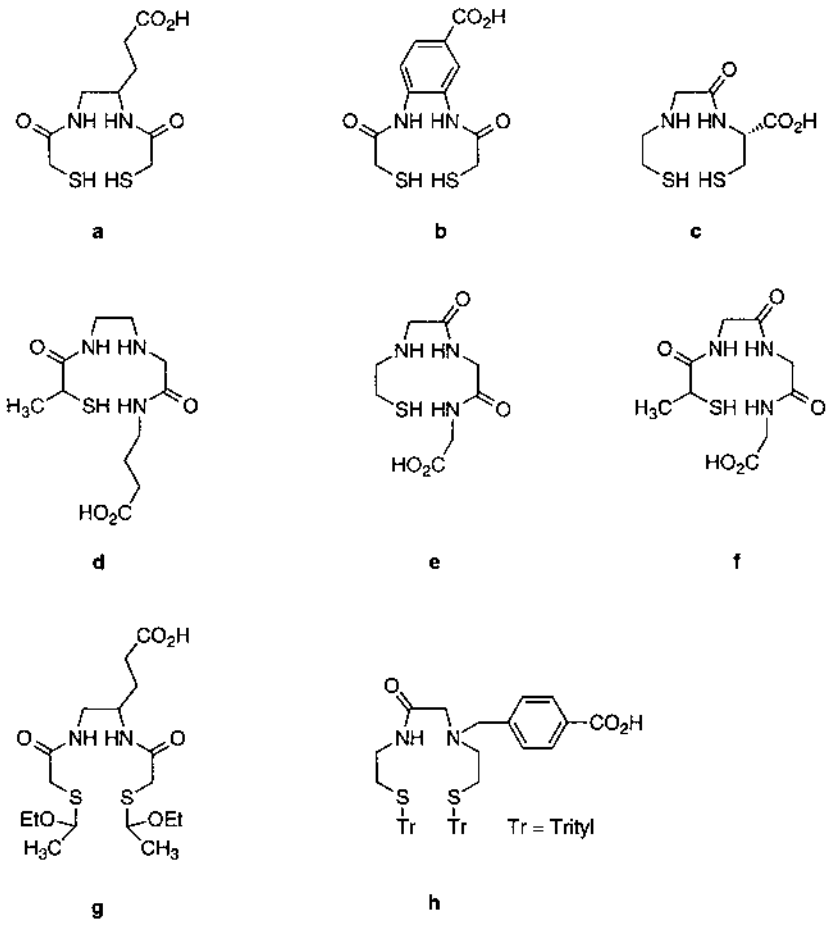

Fig. 31. Technetium binding N_2S_2 and N_3S ligands which have been conjugated to GPIIb/IIIa receptor antagonists.

system was produced containing a HYNIC ligand, a monophosphine and one tetradentate tricine co-ligand with $^{99m}TcO_4^-$. This simple reaction yielded two isomeric forms of the complex, but the exact nature of the HYNIC system and oxidation state of the metal, as stated earlier is still largely unknown. The choice of monophosphine can be tailored to alter the lipophilicity of the final radiopharmaceutical. Three analogous complexes were investigated in biological experiments, each with a different water soluble monophosphine. In each case, uptake and ability to target growing venous and arterial thrombi were not significantly different [243]. This versatile ternary ligand system has potential in producing other high-specific activity ($> 20\,000$ Ci mol^{-1}) HYNIC derivatized peptides and biomolecules.

3. MRI Agents

3.1. Introduction

Magnetic Resonance Imaging (MRI) has become one of the primary imaging modalities in modern medicine. With the widespread use of MRI has come a demand for efficient paramagnetic contrast agents, used to enhance the differences between normal and diseased tissue, or to indicate specific organ functions. The requirements for a successful MRI contrast agent are quite similar to those of a metal based radiopharmaceutical. Factors to consider include stability, charge, and lipophilicity of the metal complex. The target organ or tissue to be imaged will dictate the desired characteristics of the metal complex. For example, it is known that negatively charged compounds tend to clear through the kidney, many positively charged complexes accumulate in the heart, and an overall neutrally charged complex is required for crossing the blood–brain barrier. Lipophilic complexes will generally have more uptake in the liver and fatty tissues.

An excellent review of MRI contrast agents was published by Lauffer in 1987 [245]. A large number of reviews have appeared in the literature since then [246–259]. Future developments in this field will require the development of agents targeted to specific organs, or even specific disease states. Research has focused mostly on complexes of the paramagnetic ions gadolinium (III), iron (III), and manganese (II) due to their high magnetic moments and proton relaxivities.

Unlike most metal based radiopharmaceuticals, the ligands used to complex paramagnetic metals have a direct influence on the imaging effectiveness. The observed signal does not result from radioactive decay of the metal itself, but rather from the interaction of the metal with the aqueous environment. The choice of ligand can directly affect these interactions. The overall charge, thermodynamic and kinetic stability, lipophilicity, as well as the structure of the inner and outer solvation shells are all affected by the ligand and complex structure. In order to understand how the choice of ligand affects the functioning of an MRI contrast agent, the mechanism of proton relaxation must be understood.

Paramagnetic metal ions function as contrast agents by increasing the relaxation rates of the observed water protons near the ion, through interactions between the

electron spins of the paramagnetic center and the nuclei of the water hydrogens. The relaxivity and enhancement of proton relaxation rate can be divided into two parts: the outer sphere relaxivity (R_2) involving long range interactions with the bulk solvent, and inner sphere relaxivity (R_1) governed primarily by the exchange of water molecules bound to the paramagnetic ion with the bulk environment. The observed relaxivity is the sum of the inner and outer sphere mechanisms.

$$R_{obs} = R_1 + R_2 \tag{1}$$

The inner sphere interactions can be modeled using the Solomon–Bloembergen–Morgan (SBM) theory. A simplified version is shown in equations 2–4 [245] [260]:

$$R_1 = \left(\frac{Mq}{55.6}\right)\left(\frac{1}{T_{1M} + \tau_M}\right) \tag{2}$$

$$\frac{1}{T_{1M}} = \frac{2}{15}\gamma_H^2 g^2 \mu_B^2 S(S+1) r^{-6}\left(\frac{7\tau_c}{1+\omega_S^2\tau_c^2} + \frac{3\tau_c}{1+\omega_I^2\tau_c^2}\right) \tag{3}$$

$$\tau_c^{-1} = \tau_s^{-1} + \tau_M^{-1} + \tau_R^{-1} \tag{4}$$

where M is the concentration of the metal complex, q is the hydration number, T_{1M} is the longitudinal relaxation time, and τ_M the mean residence time of the waters on the metal center. The correlation time τ_c depends on the residence time τ_M, the electronic relaxation time τ_s, and the rotational tumbling time of the entire complex, τ_R. The remaining variables in Eq. (3) are: γ_H the proton magnetogyric ratio, g the Landè factor, μ_B the Bohr magneton, S the spin quantum number, ω_S the electronic Larmor frequency, and ω_I the proton Larmor frequency.

Improvements in the relaxivity of MRI contrast agents will depend largely on improvements in the inner-sphere relaxivity. As can be seen from Eqs. (2) and (3), several possibilities exist for improving the relaxivity. One method is to increase the correlation time, τ_c. From Eq. (4), τ_c depends on the residence time, the electronic relaxation rate, and the rotational motion of the complex. Of these, the factor most easily modified is the rotational motion. The rotational motion τ_R, is changed easily by modifying the molecular weight of the complex, most commonly by designing the compound to be conjugated to a macromolecule.

3.2. Gadolinium based agents

The literature contains many examples of gadolinium complexes proposed for use as MRI contrast agents. Rather than trying to cover all of these complexes, this review will focus on complexes currently approved for clinical use or in clinical trials. Additional discussion of gadolinium based MRI agents may be found in the paper by Yam and Lo in this issue [261]. At present three gadolinium based MRI contrast agents are currently approved for clinical use in the USA. All are polyamino carboxylate coordination complexes; two of these utilize a linear chain and the other a macrocycle. The first agent approved for clinical use in the USA by the FDA in 1988 was Gd–DTPA dimeglumine (MAGNEVIST™, gadopentetate). Another agent derived from DTPA, Gd–[DTPA–BMA], (OMNISCAN™, gadodi-

amide) is also in routine use. Recently developed agents such as Gd–[DTPA–EOB] (Schering), and Gd–BOPTA (gadobenate, Bracco) are substituted DTPA ligands, currently undergoing clinical testing. The other two agents currently approved for clinical use worldwide are macrocyclic agents based on tetraazacyclododecane, Gd–DOTA (DOTAREM™, gadoterate) and Gd–[HP–DO3A] (ProHance™, gadoteridol).

One of the main requirements of a ligand is high in vivo stability of the gadolinium complex. Free gadolinium is highly toxic and accumulates in the liver and other organs. A study of the subcellular localization found that Gd, associated with phosphate, accumulated within the lysosomes of hepatocytes and macrophages in the spleen, bone marrow and lungs [262]. Therefore, a gadolinium ligand must prevent the release of the free metal which would accumulate as $Gd(PO_4)_3$. With an appropriate choice of ligand, a gadolinium complex can be excreted from the body before the release of the free metal and concomitant toxicity.

A study published in 1990 indicated that for linear ligands a high thermodynamic stability constant alone is insufficient for predicting in vivo toxicity [263]. Cacheris and coworkers found that a more important factor was the thermodynamic selectivity of the ligand for Gd over endogenous metal ions such as Zn^{2+}, and Cu^{2+}. In particular they found transmetallation with Zn^{2+} was highly predictive of acute toxicity. A similar study published by Tweedle and coworkers looked at both linear and macrocyclic ligands [264]. They came to a similar conclusion in regards to ligand selectivity, at least for linear ligands. In the case of macrocycles the slow kinetics of transmetallation appear to outweigh any selectivity considerations.

A long term biodistribution study utilizing ^{153}Gd complexes of the commercially available gadolinium MRI contrast agents produced the most detailed distribution and clearance information for Gd complexes to date [265]. They found the biological clearance half-lives of the contrast agents ranged from 5 to 6 min in mice to 18–20 min in rats. In addition, free Gd accumulated primarily in the liver and bone and cleared from the body at a rate of 1–3% per day. The complex stability in vivo paralleled the rates of complex dissociation under acidic conditions. This is most likely due to the complexes being hydrolyzed within the lysosomes [266].

As mentioned previously, all of the clinically approved gadolinium MRI contrast agents are based on aminocarboxylate type ligands. This choice of ligand type has a direct effect on the complex's effectiveness at increasing the relaxation rate of the inner sphere water molecules. From Eq. (4) we see that the correlation time (τ_c) is related to the residence time (τ_m) of a water molecule bound to the paramagnetic center. This residence time is equivalent to $1/k_{ex}$, where k_{ex} is the exchange rate constant. Until recently, the rate of water exchange of Gd(III) based contrast agents was assumed to be approximately the same as that found for the Gd(III) aqua complex ($(8.3 \pm 1.0) \times 10^8\ s^{-1}$) [267]. In a series of variable temperature and pressure NMR studies, Pubanz and coworkers found that the water exchange rates, k_{ex}, for Gd complexes of DTPA and DOTA were actually two orders of magnitude lower (Gd–DTPA k_{ex} $(4.1 \pm 0.3) \times 10^6\ s^{-1}$; Gd–DOTA k_{ex} $(4.8 \pm 0.4) \times 10^6\ s^{-1}$) [268]. These data show that the presence of the aminocarboxylate groups affect the rate of exchange compared with that of the aqua complex.

In a more recent study, Pubanz found that waters exchange via a dissociative mechanism with Gd–[DTPA–BMA], and it was speculated that the exchange rate is controlled by the ligand steric requirements at the water binding site [268]. If true, by modifying the steric environment of the ligand, the exchange rate could be regulated upwards increasing the overall relaxivity.

At relatively high magnetic field strengths, compounds of similar size and mass, and therefore diffusion rate, have approximately the same outer sphere (R_2) contributions. Tweedle and coworkers verified this experimentally for a series of linear and macrocyclic amino carboxylate complexes; at 0.47 T and 40°C, they found an average R_2 value of 2.0 ± 0.3 (mM s)$^{-1}$ [269,270]. This means that for Gd(III) complexes with identical values of q, any differences in relaxivities will be due to differences in the inner sphere contribution R_1. Aime and coworkers have found a correlation between the molecular weight of the Gd complex and the inner sphere relaxivity R_1 [271,272].

In most poly(amino) carboxylates the major factor determining R_1 is the correlation time τ_c. This value is determined by the fastest of τ_s, τ_M, and τ_R; with τ_R usually being the fastest. One exception is observed with bis(amide) complexes, in these τ_M is seen to control the relaxivity.

Aime et al. investigated the magnetic field dependence of the water relaxation rate of Gd–[DTPA–BMA] and found that τ_M was approximately four-fold longer than τ_M of Gd–DTPA; this increase was enough to make the contribution of τ_M significant [260]. They postulated two explanations for this lengthening of τ_M. One is the presence of an extended three dimensional network of hydrogen bonded waters between the amides and the carboxylate groups. Alternatively, the presence of the amide groups may affect the partial atomic charge on the Gd, resulting in the increase of τ_M.

3.2.1. Open chain ligands

3.2.1.1. Gd–DTPA (MAGNEVIST™, gadopentetate). In 1984 the gadolinium complex of DTPA (Fig. 10b) was first evaluated as an MRI contrast agent [273]. In comparison to the gadolinium aquo complex, the relaxivity of Gd–DTPA is significantly lower (see Table 4). However, the toxicity of free gadolinium was believed to be moderated by the strong complexation of the eight-coordinate DTPA ligand. The LD_{50} in rats of $GdCl_3$ was found to be 0.5 mmol kg^{-1}, while the LD_{50} of GdDTPA was 10 mmol kg^{-1} [273]. The overall charge for the complex is -2, thus two equivalents of the positively charged meglumine salt ($+1$) were utilized as counterions. As Gd(III) aquo complexes are believed to be nine- or ten-coordinate, DTPA leaves a vacant coordination site for binding an inner sphere water molecule. An X-ray structure of the complex was obtained and found to be a distorted capped square antiprism, with a water molecule forming the cap on the square antiprism [274].

The initial animal studies utilizing rats and dogs showed promising behavior of Gd–DTPA with rapid clearance through the kidneys [275]. A later study examined the biodistribution of radiolabeled ^{153}Gd–DTPA in mice and came to the same conclusions as to rate and mode of clearance from the body [276].

Table 4
MRI contrast agents (all values of R_1 measured at 20 MHz)

Complex	Log K	q	Charge	R_1 (mM^{-1} s^{-1})	Ref.
Gd-$[H_2O]_9$		9	+3	9.1 (37°C)	[245]
Gd–DTPA	22.39	1	−2	3.7 (37°C)	[245,348]
Gd–[DTPA–BMA]	16.9	1	0	3.8 (40°C)	[252]
Gd–[DTPA–EOB]		1	2	5.3 (37°C)	[285]
Gd–BOPTA	22.59	1	−2	4.39 (39°C)	[272]
Gd–DOTA	24	1	−1	3.4 (37°C)	[348,349]
Gd–DO3A	21	1.8	0	4.85 (40°C)	[269,308]
Gd–[HP–DO3A]	23.8	2	0	3.65 (40°C)	[269,308]
Fe–EHPG	35.54	0	−1	0.95 (37°C)	[102,245]
Mn–DPDP	15.10	0	−2	2.4[a] (37°C)	[326,327]

[a] R_1 measured at 10 MHz.

The first human imaging trials of Gd–DTPA dimeglumine were conducted in 1984 by Laniado [277]. The pharmacokinetics of Gd–DTPA were studied and reported by Weinmann in the same year [278]. Further MRI studies on humans were reported in 1994 by Carr and coworkers [279,280]. In short, after IV injection of Gd–DTPA the complex rapidly diffuses throughout the vascular system, and is predominately excreted unmetabolized through the renal system [278]. A relatively recent review of clinical applications of Gd–DTPA was published by Bydder in 1991 [250].

3.2.1.2. Gd–[DTPA–BMA] (OMNISCAN™, gadodiamide). Gd–[DTPA–BMA] (Fig. 32a) is a second generation MRI contrast agent designed to improve the in vivo behavior of Gd–DTPA [252]. The first reported synthesis of Gd–[DTPA–BMA] was in 1984 [281]. By converting two of the carboxylates into methyl amides the overall charge of the gadolinium complex is reduced to zero. This has the advantage of greatly reducing the osmolality which lowers the risk of physiological complications. The normal osmolality of blood and extracellular fluid is 290 mmol

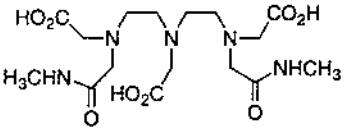

a) DTPA - BMA

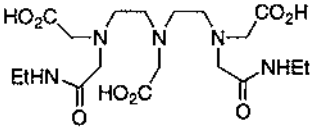

b) DTPA - BEA

Fig. 32. Bis(alkylamide) derivatives of DTPA.

kg^{-1}, the osmolality of Gd–DTPA dimeglumine is 1940 mmol kg^{-1}, in contrast the osmolality of gadodiamide is 789 mmol kg^{-1} [252].

A crystal structure of the closely related Gd–[DTPA–BEA], or bis(ethyl)amide (Fig. 32b) was reported in 1990 [282]. The gadolinium was nine-coordinate with eight sites taken by the ligand and a water molecule filling the ninth. The coordination geometry was found to be a distorted tricapped trigonal prism. The amide oxygens were clearly shown to be involved in bonding to the gadolinium by shortening of the Gd–O bonds, with IR evidence providing further proof.

The in vivo stability and behavior of Gd–[DTPA–BMA] was first investigated by Cacheris and coworkers in 1990 [263]. Despite the replacement of two carboxylate ligand groups with two amides it was found that Gd–[DTPA–BMA] released about one-half as much Gd(III) as did Gd–DTPA. This resulted in a greater than two-fold increase in LD_{50} values in mice (Na_2[Gd–DTPA] 5.6 mmol kg^{-1}, and Gd–[DTPA–BMA] 14.8 mmol kg^{-1}). The replacement of two carboxylates with two amide groups was found to have a small effect on the relaxivity, as seen in Table 4.

Pharmacokinetic studies found that the complex did not cross the blood brain barrier and cleared primarily through the kidneys similarly to Gd–DTPA [283]. Phase I human clinical trials were first reported in 1993, and concluded that Gd–[DTPA–BMA] was a promising MRI contrast agent [284].

3.2.1.3. Gd–[DTPA–EOB]. Another second generation MRI contrast agent, Gd–[DTPA–EOB] targets a specific organ, the liver, rather than improving on the physicochemical behavior of DTPA. The liver is a major focus for development of new agents due to the clinical usefulness of detecting and characterizing hepatic lesions. The ligand (Fig. 33) is a derivative of DTPA with a 4-ethoxybenzyl group on the ethylene bridge backbone. Initial biodistribution studies of the complex found that unlike the previous DTPA based agents, the primary mode of clearance was through the liver into the bile and feces [285]. As shown in Table 4, Gd–[DTPA–EOB] has a large T_1 relaxivity (5.3 mM^{-1} kg^{-1}); in liver tissue this rises to 16.9 mM^{-1} kg^{-1} [285]. The high liver relaxivity is believed due to an increase in viscosity as well as specific interactions with transport proteins such as glutathione-*S*-transferase, and nonspecific interactions with other proteins [286]. This increased relaxivity has the potential of lowering the effective dose of contrast agent required for a given signal enhancement.

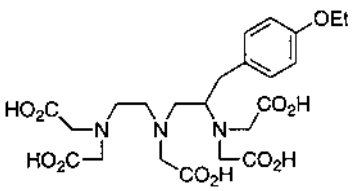

DTPA-EOB

Fig. 33. Structure of DTPA–EOB, whose Gd(III) complexes targets the liver.

In animal studies, Gd–[DTPA–EOB] was distributed throughout the extracellular fluid space and was taken up by hepatocytes with ultimate elimination through the bile [286–288]. Schuhmann-Giampieri and coworkers found that the hepatocyte uptake involved both the albumin-binding organic anion transport system, and the intracellular transport protein glutathione-*S*-transferase [286].

Phase I clinical trials were reported in 1995 and gave a favorable in vivo safety profile [289]. Latter trials were reported in 1996 and 1997 and reported the same findings [290,291]. Unlike animal models, in humans Gd–[DTPA–EOB] was cleared from the body equally through the urine and bile. From imaging studies at later timepoints, only the liver and kidney showed significant enhancement [289].

3.2.1.4. Gd–BOPTA (gadobenate). First reported in 1988 by Vittadini and coworkers [292], Gd–BOPTA possesses a lipophilic aromatic group, in this case a benzyloxymethyl group (Fig. 34) which appeared to impart a high liver uptake of the complex, similar to DTPA–EOB. A synthetic procedure and X-ray structure of the Gd–BOPTA complex was reported in 1995, and two enantiomeric forms of the complex were found in the unit cell [272]. As expected, the gadolinium is nine coordinate in a distorted tricapped trigonal prism, with a water molecule occupying the ninth coordination site.

Initial animal studies found that this compound was rapidly distributed throughout the extracellular space and showed modes of clearance similar to that of Gd–[DTPA–EOB], with 54.8% clearing through the kidneys and 38.6% the liver [292]. The relaxivity of this compound was lower than Gd–[DTPA–EOB] (Table 4) and showed a similar enhancement in the liver. Again, this is thought to be due to a combination of factors such as increased viscosity and interactions with proteins. The complex displayed a leveling off of the liver signal enhancement with increased amounts of Gd–BOPTA suggesting a saturation of the biliary excretion pathway [293].

Initial phase I clinical trials were reported in 1991 and found the complex to be safe and effective for liver imaging [294]. It was suggested that GdBOPTA could serve a dual purpose in liver imaging: immediately after injection it characterizes perfusion, and at later time points shows functional liver tissue via uptake by functioning hepatocytes [295]. At present, phase II clinical trials have been reported with no evidence of adverse effects [295,296].

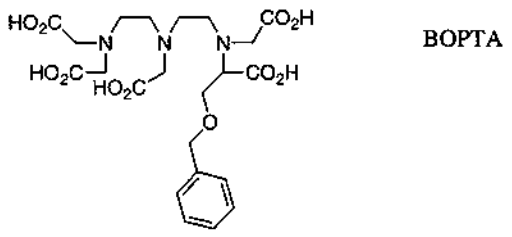

BOPTA

Fig. 34. Structure of BOPTA, an additional liver imaging agent for Gd(III).

3.2.2. Macrocyclic ligands

3.2.2.1. Gd–DOTA (Dotarem™, gadoterate). The gadolinium complex of the eight-coordinate macrocyclic ligand DOTA (Fig. 14b) was first evaluated as an MRI contrast agent in 1986 [297,298]. At present it is approved for clinical use in several European countries. As has already been mentioned, the macrocyclic Gd(III) complexes have a much lower toxicity than the open chain ligands; in one study the LD_{50} in mice of Gd–DOTA was found to be 93% higher than that of Gd–DTPA [299]. Two separate reports of the solid state structure have appeared in the literature. In both cases the Gd(III) is nine coordinate in a square antiprismatic arrangement with a water molecule at the ninth coordination site [300,301].

Similar to Gd–DTPA, the negatively charged Gd–DOTA complex distributes rapidly throughout the extracellular space and rapidly clears through the kidneys [276,299]. The complex has a relaxivity slightly lower than that of Gd–DTPA, Table 4. Phase I clinical trials were reported in 1990 with no adverse effects noted [302]. Later clinical trials arrived at the same conclusion [303].

3.2.2.2. Gd–DO3A. The ligand DO3A (Fig. 35), while not approved for clinical use, has been extensively studied and deserves mention. This ligand was the first to serve as a neutral macrocyclic chelate for gadolinium, and can be compared to DTPA–BMA, a neutral open chain ligand. The first reported synthesis of DO3A was in 1988 with a more detailed procedure being published in 1991 [304,305]. The crystal structure of the Gd complex was reported in 1993 [301]. The ligand provides a seven-coordinate environment for the gadolinium leaving two sites open for coordinating waters, in the unit cell these sites are filled by a single carbonate ion binding in a bidentate fashion.

Despite only having seven coordination sites, the thermodynamic stability constant of Gd–DO3A is still significantly higher than that of Gd–[DTPA–BMA], as can be seen in Table 4. The loss of a carboxylate group when compared to DOTA lowers the thermodynamic stability by three log units; however, the complex displays a high degree of kinetic inertness due to the rigidity of the cyclen backbone [264]. The complex has a relaxivity higher than both Gd–DOTA and Gd–DTPA (Table 4). It was evaluated as an MRI contrast agent in rats and found to be very similar to Gd–DOTA and Gd–DTPA [306]. Despite the initial promise of this ligand it was rapidly replaced by the ligand HP–DO3A.

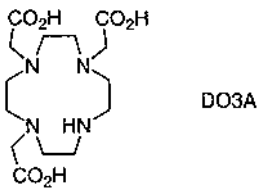

Fig. 35. The macocyclic ligand DO3A.

3.2.2.3. Gd–[HP–DO3A] (ProHance™, gadoteridol). The first reported synthesis of this macrocyclic ligand was in 1991 [305]. This derivative of DO3A has the free backbone nitrogen alkylated by a 2-hydroxypropyl group (Fig. 36). The potentially ionizable hydroxy group, under physiological conditions remains protonated, resulting in an overall neutral charge for the gadolinium complex [307]. Despite remaining protonated, the hydroxy group binds to Gd(III) leaving the ligand eight-coordinate. The crystal structure was reported in 1994; the metal is nine-coordinate with the ligand filling eight sites and a water molecule filling the ninth position [308]. The addition of the hydroxy group raises the thermodynamic stability constant (Table 4) by almost two log units compared to DO3A bringing the stability constant to just below that of DOTA. The relaxivity however, was lower than that measured for Gd–DO3A.

Initial preclinical animal studies found that Gd–[HP–DO3A] was less toxic than Gd–DTPA and looked promising as an MRI contrast agent [309]. The complex distributed rapidly throughout the extracellular space and was cleared quickly through the kidneys [265]. A comparison of the physiochemical properties of Gd–[HP–DO3A], Gd–DTPA, Gd–[DTPA–BMA], and Gd–DOTA showed that the best combination of properties for an MRI agent were the presence of a macrocyclic backbone and low osmolality, both of which were found in the ligand HP–DO3A [307]. The favorable properties of Gd–[HP–DO3A] led to rapid clinical trials.

The results of phase I clinical trials were reported in 1991 [310,311]. The complex was found to be safe and effective as a contrast agent. Phase II and phase III trials were reported soon after with similar results [312–315].

3.3. Iron based agents

Paramagnetic complexes of iron and manganese have also been utilized as MRI contrast agents. Many ligands that complex Gd(III) will also form stable complexes with both Fe(III) and Mn(III). However, most of the ligands used to bind Gd(III) are eight-coordinate, but both Mn(III) and Fe(III) usually form six-coordinate complexes. It is therefore unlikely that water molecules can coordinate directly to the paramagnetic center with ligands such as DTPA or DOTA. This lowers the T_1 relaxivity to much lower levels than the corresponding gadolinium complexes. As an example, Fe(III)DTPA has an R_1 value of 0.7 mM^{-1} s^{-1} at 20 MHz and 39°C,

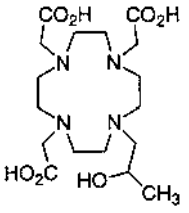

HP-DO3A

Fig. 36. The macrocyclic ligand HP–DO3A.

while Fe(III)DOTA has an R_1 of 0.4 mM^{-1} s^{-1} under similar conditions [316]. When compared to the gadolinium values in Table 4, we see that these complexes are much less effective. In order to have a comparable effectiveness, ligands for iron and manganese have to be of a lower denticity than those utilized with Gd(III).

An alternative approach for iron based MRI contrast agents is the use of ultrasmall paramagnetic iron oxide particles [250,317,318]. These function as T_2 contrast agents as opposed to the T_1 agents discussed previously. These particles of synthetic magnetite (Fe_3O_4) are typically mixtures of magnetite, maghemite (Fe_2O_3), and hematite (Fe_2O_3), and are sometimes accompanied by hydrated iron oxides [319]. As such these compounds do not fit the definition of a coordination compound as used in this review.

3.3.1. Fe–HBED and Fe–EHPG

Two iron complexes evaluated as MRI contrast agents are Fe(III)EHPG and Fe(III)HBED [320–322]. These ligands (Fig. 13a and Fig. 12a) have been shown to form stable complexes with Ga(III) and In(III) (Section 2.5.3), but are also good ligands for Fe(III). The Fe(III) complexes were found to serve as hepatobiliary contrast agents, and are substrates for the organic anion transport system within the liver; as are Gd–BOPTA and Gd–[DTPA–EOB] [249]. The X-ray structure of Fe–EHPG was reported by Bailey and coworkers in 1981; the iron was found to be six-coordinate in an octahedral arrangement [323]. The hexadentate ligand fills all of the available coordination sites, leaving no sites for binding water molecules. Unlike the gadolinium agents discussed previously, the observed relaxivity of this complex must arise from the outer sphere R_2 mechanism. The effect of this can be seen in the relaxivity values reported in Table 4. In animal imaging experiments, Lauffer et al. found that the agent improved significantly the liver images, despite the fact that the negatively charged complex cleared primarily through the renal system [320,321].

Lauffer and coworkers have also examined derivatives of Fe–EHPG substituted in the 5-position with methyl, chloro, or bromo for their hepatobiliary behavior and binding to the blood protein human serum albumin (HSA) [324,325]. Interestingly, these very similar complexes displayed pharmacokinetic differences; the complexes of Fe–[5-BrEHPG] even displayed differences among its diastereomers [325].

3.4. Manganese based agents

Paramagnetic complexes of Mn(III) are also useful as MRI contrast agents. As in the case of iron, many ligands that complex Gd(III) also form stable complexes with Mn(III). The use of Mn(III) generally requires the use of six-coordinate ligands in order to ensure high thermodynamic stability; however, with the ligand filling all of the available coordination sites, water molecules are unable to coordinate directly to the paramagnetic center. This means that these complexes, as with the previously discussed Fe(III) agents, have to function through the outer sphere mechanism. To date only one Mn(III) based agent is undergoing clinical trials.

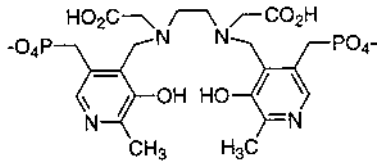

DPDP

Fig. 37. The manganese ligand DPDP.

3.4.1. Mn–DPDP (manganese dipyridoxyl diphosphate)

This complex was first synthesized and characterized in 1989 [326]. The ligand DPDP (Fig. 37) is a water soluble hexadentate ligand similar to the ligand PLED, derived from pyridoxal-5′-phosphate. The manganese coordination was found to be a distorted octahedron with the ligand filling all of the coordination sites. With no sites for the direct coordination of water to the paramagnetic center, this complex like Fe–EHPG functions primarily through the outer sphere relaxation R_2 mechanism.

Preclinical and phase I clinical trials of Mn–DPDP were reported in 1990 [327]. The agent was found to target the liver and in rats radiolabeled ^{54}Mn–DPDP was found to have 47% hepatobiliary clearance and 43% renal clearance. This compares quite favorably to other liver agents such as Gd–BOPTA and Gd–[DTPA–EOB] both of which have lower liver targeting. The toxicity was found to be acceptable for clinical use although it was higher than that of Gd–DTPA. In mice, the LD_{50} of Mn–DPDP was 1.9 mmol kg^{-1} while the LD_{50} of Gd–DTPA was 10.6 mmol kg^{-1} [299,327]. The phase I trials found no clinically significant drug or dose related reactions. MRI liver signal enhancements were observed as early as 1 min post-injection and lasted as long as 30 min. In addition to targeting the liver, Mn–DPDP was found to be effective at evaluating myocardial ischemia in rats [328].

Phase II clinical trials were conducted both in the USA and Germany [329,330]. A review of the clinical studies appeared in 1992 [331]. In both studies Mn–DPDP was found to be effective as an MRI contrast agent and safe at the doses required for MRI. The only side effect in the studies was a momentary facial flushing after injection.

3.5. Macromolecular conjugates

As with radiopharmaceuticals (Section 2.8) MRI contrast agents can be attached to other molecules, both biological and synthetic, to target specific receptor systems in vivo, or to improve their relaxivities. In most cases the bifunctional chelate utilized has been DTPA or a closely related derivative. All of the MRI contrast agents discussed thus far have been extracellular agents, diffusing from the intravascular system and distributing rapidly thoroughout the body. In some studies it

would be desirable to have an intravascular agent, which would remain solely in the blood pool [332]. This can be accomplished by increasing the molecular weight of the contrast agent to above 20 000 Da (Gd–DTPA has a molecular weight of 545 Da). At this size, the agents remain within the intravascular space for a much longer period of time. A common approach to increasing the mass of a paramagnetic complex such as Gd–DTPA, is to conjugate the complex to a high molecular weight polymer. Some polymers which have been utilized for this purpose are albumin, dextran, and polylysine [332].

Confining the contrast agent to the vascular system is not the sole benefit to using polymeric paramagnetic complexes. By attaching one or more paramagnetic complexes to a polymer the relaxivity can be greatly enhanced over that of the monomeric species. From Eq. (4) we see that the correlation time t_c and ultimately the T_1 relaxivity, depends on the rotational tumbling time of the entire complex, t_R. Increasing the molecular weight of the paramagnetic complex will primarily slow the rotational tumbling time t_R. When the tumbling rate can be slowed to ca. 10^{-8} s the relaxivity will be enhanced, this generally requires increasing the molecular weight to above 10 000 Da [332].

A recent example of such a MRI contrast agent results from the coupling of a DTPA derivative MX–DTPA (Fig. 38) [333] to a Starburst™ dendrimer [334]. A Starburst™ dendrimer is a virtually monodisperse polymer; starting with ammonia an iterative cycle of methylacrylate addition followed by reaction with ethylenediamine rapidly builds a polyamidoamine polymer with an outer surface containing reactive amines. The two dendrimers utilized in this study were of generation 2, two reaction cycles, and generation 6, six cycles. These had 12 and 192 reactive amines, respectively, available for attaching the bifunctional chelate. The generation 2 dendrimer chelate conjugate was found to bind 11 Gd(III) ions, and possessed a relaxivity of 234 mM s^{-1} at 25 MHz and 20°C. The generation 6 dendrimer chelate conjugate was found to bind 170 gadolinium ions, and possessed a relaxivity of 5800 mM s^{-1} at 25 MHz and 20°C.

While attaching paramagnetic metals with BFCs to non-specific plasma proteins like HSA to lengthen blood retention times and increase the relaxivity, using BFCs to label organ or tissue specific biomolecules offers another way of targeting the

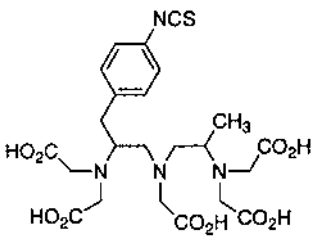

MX - DTPA

Fig. 38. The bifunctional chelate MX–DTPA.

imaging agent. One such type of tissue specific biomolecule are monoclonal antibodies.

Labeling antibodies with paramagnetic complexes allows the targeting of tumors, potentially improving the ability of MRI to detect smaller tumors and improve the contrast between normal and diseased tissue. In a theoretical study of the expected target to non-target ratio (antigen bound vs free antibody) for a radiolabelled antibody of M_w 150 000 Da, it was found that the target to non-target ratio drops significantly when large amounts of anitibody are used [335]. In an ideal case, the total concentration of antibody bound to the tumor antigen would be less than 10^{-7} M. If each molecule of antibody were labeled with one atom of gadolinium, the concentration of contrast agent in the tumor would be 10^{-7} M. On current MRI scanners, the required dose of Gd–DTPA for successful image enhancement results in a concentration of Gd–DTPA throughout the body of 10^{-4} M, three orders of magnitude above what could be achieved with a mono-labeled antibody [336]. One solution to this concentration problem would be to label antibodies with more than one paramagnetic complex. A study by Unger and colleagues found that in order to get a useful concentration of Gd(III) into a tumor, a typical antibody would have to labeled with 2424 molecules of Gd–DTPA, requiring every amino acid of the antibody to be labeled with several DTPA ligands [337]. This would appear to be an impossible task, since even if the coupling of the bifunctional chelate to the antibody went in 100% efficiency, the immunoreactivity would surely be compromised.

A possible solution to this situation is the use of polychelates which results in many paramagnetic complexes being conjugated to each labelling site [338]. Using this method, polylysine was conjugated with both DTPA and DOTA, resulting in sixty to ninety chelating groups per molecule of polylysine (the polychelate). The functionalised polylysine was then complexed with Gd(III) followed by coupling to HSA. This procedure resulted in HSA labeled with 60–90 mol of gadolinium per mole of protein. This is a significant improvement in labeling efficiency, and in some cases it might be possible to attach more than one polychelate per protein. In addition to improved conjugation efficiencies, the polychelates were found to have relaxivities 2.5 times greater than the monomeric gadolinium complexes.

In the preceding sections (Sections 3.2.1, 3.3.1 and 3.4.1) several MRI contrast agents which targeted the liver were presented: Gd–[DTPA–EOB], Gd–BOPTA, Fe–EHPG, and Mn–DPDP. Using bifunctional chelates allows another approach to targeting specific organs. Proteins are not the only type of biomolecule which can be congugated to BFCs; Mühler and coworkers attached Gd–DO3A, a non-specific extracellular agent, to cholesterol in order to image the liver and adrenals [339]. More than 99% of the conjugate was found to be protein bound in serum, which could explain the observed differences in relaxivities (R_1) 17.9 mM^{-1} s^{-1} in water and 21.2 mM^{-1} s^{-1} in serum, both at 20 MHz and 40°C. These are significantly higher than the measured relaxivity (R_1) of Gd–DO3A in water at 20 MHz and 40°C of 4.85 mM^{-1} s^{-1} [269]. The bioconjugate complex was found to accumulate in both the adrenal gland and liver similar to natural cholesterol. The observed MRI enhancements after injection were found to be 162% in the adrenals and 146% in the liver.

4. Summary and conclusion

It is clear from this review that the use of metal complexes in gamma scintigraphy, PET and MRI is a rapidly growing area of research. During the past 10 years, countless agents have been developed, evaluated in animal models and are either currently in clinical trials or are approved for clinical use in the USA for use in diagnostic imaging of disease. This review has attempted to highlight the metal complexes that have been synthesized and evaluated in vivo over the last 10 years.

Along with major advances in the chemical synthesis and coordination chemistry of new ligands and metal complexes, significant strides have been made in correlating physical characteristics of metal complexes with biological behavior. Metal complexes are currently being utilized in the diagnosis of a wide variety of disease states ranging from heart disease, brain disorders, and cancer. Metal complexes are also able to determine specific aspects of disease such as tissue hypoxia, as well as detect molecular phenomena such as multi-drug resistance. The advent of attaching metal complexes to larger biological molecules has essentially created a new realm of research in the field of bioconjugates. Metal complexes attached to biomolecules allow even more specific biological processes to be studied, including the formation of thrombi, the imaging of infection, and the understanding of antigens and receptors found in certain types of cancer to name a few examples.

One of the goals of this review is to educate coordination chemists to the wide number of applications of our field to biology, physics and medicine, to learn from all the previous research and design better agents to aid in the diagnosis and understanding of more disease states. In reflecting on the enormous amount of progress made just in the past 10 years, it is apparent that by working with each other along with biologists, physicists and physicians, there is no limit to what can be accomplished.

Acknowledgements

The authors gratefully acknowledge financial support from the National Cancer Institute, Department of Energy, and Mallinckrodt, Inc. The authors would also like to acknowledge the scientists who have devoted their careers to doing research in the interface between inorganic chemistry and diagnostic imaging.

References

[1] H.M. Chilton, R.L. Witcofski, Pharmaceuticals in Medical Imaging, Macmillan Publishing, New York, 1990.
[2] M.K. Dewanjee, Semin. Nucl. Med. 20 (1990) 5.
[3] S. Jurrison, D. Berning, W. Jia, D. Ma, Chem. Rev. 93 (1993) 1137.
[4] T.R. Carroll, Adv. Met. Med. 1 (1993) 1.
[5] B.A. Rhodes, Int. J. Radiat. Appl. Instrum.-Part B, Nucl. Med. Biol. 18 (1991) 667.
[6] A.J. Fischman, J.W. Babich, R.H. Rubin, Sem. Nucl. Med. 24 (1994) 154.

[7] W.C. Eckelman, Eur. J. Nucl. Med. 22 (1995) 249.
[8] M.L. Thakur, Nucl. Med. Commun. 16 (1995) 724.
[9] T.M. Behr, D.M. Goldenberg, J. Nucl. Med. 37 (1996) 834.
[10] J. Lister-James, B.R. Moyer, T. Dean, Quart. J. Nucl. Med. 40 (1996) 221.
[11] E.C. Constable, C.E. Housecroft, Coord. Chem. Rev. 131 (1994) 153.
[12] F. Tisato, F. Refosco, G. Bandoli, Coord. Chem. Rev. 135/136 (1994) 325.
[13] C.E. Housecroft, Coord. Chem. Rev. 142 (1995) 21.
[14] C.E. Housecroft, Coord. Chem. Rev. 146 (1995) 191.
[15] J.R. Riordan, K. Deuchars, N. Kartner, N. Alon, J. Trent, V. Ling, Nature 316 (1983) 817.
[16] G. Bradley, P.F. Juranka, V. Ling, Biochim. Biophys. Acta 948 (1988) 87.
[17] R.L. Juliano, V. Ling, Biochim. Biophys. Acta 455 (1976) 152.
[18] N. Kartner, J.R. Riordan, V. Ling, Science 221 (1983) 1285.
[19] S.P.C. Cole, G. Bhardwaj, G.H. Gerlach, J.E. Mackie, C.E. Grant, K.C. Almquist, et al., Science 258 (1992) 1650.
[20] P.A. Carvalho, M.L. Chiu, J.F. Kronauge, M. Kawamura, A.G. Jones, B.L. Holman, et al., J. Nucl. Med. 33 (1992) 1516.
[21] P. Gros, F. Talbot, D. Tang-Wai, E. Bibi, H.R. Kaback, Biochemistry 31 (1992) 1992.
[22] A.G. Jones, M.J. Abrams, A. Davison, J.W. Brodack, A.K. Toothaker, S.J. Adelstein, et al., Int. J. Nucl. Med. Biol. 11 (1984) 225.
[23] D. Piwnica-Worms, B.L. Holman, J. Nucl. Med. 31 (1990) 1166.
[24] D. Piwnica-Worms, M.L. Chiu, M. Budding, J.F. Kronauge, R.A. Kramer, J.M. Croop, Cancer Res. 53 (1993) 977.
[25] D. Piwnica-Worms, V.V. Rao, J.F. Kronauge, J.M. Croop, Biochemistry 34 (1995) 12210.
[26] J.R. Ballinger, H.A. Hua, B.W. Berry, P. Firby, I. Boxen, Nucl. Med. Commun. 16 (1995) 253.
[27] M.D. Cordobes, A. Starzec, L. Delmon-Moingeon, C. Blanchot, J.C. Kouyoumdjian, G. Prevost, et al., J. Nucl. Med. 37 (1996) 286.
[28] I. Bosch, C.L. Crankshaw, D. Piwnica-Worms, J.M. Croop, Leukemia 11 (1997) 1131.
[29] S. Del-Vecchio, A. Ciarmiello, L. Pace, M.I. Potena, M.V. Carriero, C. Mainolfi, et al., J. Nucl. Med. 38 (1997) 1348.
[30] G.D. Luker, P.M. Fracasso, J. Dobkin, D. Piwnica-Worms, J. Nucl. Med. 38 (1997) 369.
[31] L.W. Herman, V. Sharma, J.F. Kronauge, E. Barbarics, L.A. Herman, D. Piwnica-Worms, J. Med. Chem. 38 (1995) 2955.
[32] C. Rossetti, G. Paganelli, G. Vanoli, C. Di Leo, M. Kwiatkowski, F. Zito, et al., J. Nucl. Biol. Med. 36 (1992) 29.
[33] C. Rossetti, G. Vanoli, G. Paganelli, M. Kwiatkowski, F. Zito, F. Colombo, et al., J. Nucl. Med. 35 (1994) 1570.
[34] C.L. Crankshaw, M. Marmion, B.D. Burleigh, E. Deutsch, D. Piwnica-Worms, J. Nucl. Med. 36 (1995) 130P.
[35] C.L. Crankshaw, M. Marmion, G.D. Luker, V. Rao, J. Dahlheimer, B.D. Burleigh, et al., J. Nucl. Med. 39 (1998) 77.
[36] J.D. Kelly, A.M. Forster, B. Higley, C.M. Archer, F.S. Booker, L.R. Canning, et al., J. Nucl. Med. 34 (1993) 222.
[37] B. Higley, F.W. Smith, T. Smith, H.G. Gemmell, H.G. Das Gupta, D.V. Gvozdanovic, et al., J. Nucl. Med. 34 (1993) 30.
[38] J.R. Ballinger, J. Bannerman, I. Boxen, P. Firby, N.G. Hartman, M.J. Moore, J. Nucl. Med. 37 (1996) 1578.
[39] C.N. Coleman, J. Natl. Cancer Inst. 80 (1988) 137.
[40] K.E. Linder, Y.W. Chan, J.E. Cyr, D.P. Nowotnik, W.C. Eckelman, A.D. Nunn, Bioconjugate Chem. 4 (1993) 326.
[41] K.E. Linder, Y.W. Chan, J.E. Cyr, M.F. Malley, D.P. Nowotnik, A.D. Nunn, J. Med. Chem. 37 (1994) 9.
[42] W.L. Rumsey, J.E. Cyr, N. Raju, R.K. Narra, Biochem. Biophys. Res. Commun. 193 (1993) 1239.
[43] W.L. Rumsey, B. Patel, K.E. Linder, J. Nucl. Med. 36 (1995) 632.
[44] C.K. Ng, A.J. Sinusas, B.L. Zaret, R. Soufer, Circulation 92 (1995) 1261.

[45] R.D. Okada, K.N. Nguyen, H.W. Strauss, G.R. Johnson, Eur. J. Nucl. Med. 23 (1996) 443.
[46] J.R. Ballinger, J.W. Kee, A.M. Rauth, J. Nucl. Med. 37 (1996) 1023.
[47] R.D. Okada, G. Johnson, K.N. Nguyen, B. Edwards, C.M. Archer, J.D. Kelly, Circulation 85 (1997) 1892.
[48] R.D. Okada, K.N. Nguyen, M. Lauinger, I.L. Allton, G.R. Johnson, Am. Heart. J. 132 (1996) 108.
[49] S.A. Cotton, F.A. Hart, The Heavy Transition Metals, Macmillan Press, London, 1975.
[50] E. Deutsch, K. Libson, J.-L. Vanderheyden, A.R. Ketring, H.R. Maxon, Nucl. Med. Biol. 13 (1986) 465.
[51] J.M. de Klerk, A. van Dijk, A.D. van het Schip, B.A. Zonnenberg, P.P. van Rijk, J. Nucl. Med. 33 (1992) 646.
[52] J.M. de Klerk, A.D. van het Schip, B.A. Zonnenberg, A. van Dijk, J.M. Quirijnen, G.H. Blijham, et al., J. Nucl. Med. 37 (1996) 244.
[53] D.C. Bradley, Prog. Stereochem. 3 (1962) 1.
[54] N.N. Greenwood, Adv. Inorg. Chem. Radiochem. 5 (1963) 91.
[55] D.G. Tuck, Gallium and Indium, vol. 1, Pergamon Press, Oxford, 1982.
[56] M.A. Green, M.J. Welch, Nucl. Med. Biol. 16 (1989) 435.
[57] C.J. Anderson, M.J. Welch, Gallium, in: H.G. Seilor, A. Siegel, H. Siegel (Eds.), Handbook on Metals in Clinical and Analytical Chemistry, Marcel Dekker, Basel, 1994.
[58] H.D. Bruner, R.L. Hayes, J.D.X. Perkinson, Radiology 61 (1953) 602.
[59] C. Loc'h, B. Mazièré, D. Comar, J. Nucl. Med. 21 (1980) 171.
[60] P. Goethals, M. Coene, G. Slegers, P. Agon, J. Deman, K. Schelstraete, Eur. J. Nucl. Med. 14 (1988) 152.
[61] M.E. Daube-Witherspoon, S.L. Green, P. Plascjak, C. Wu, R.E. Carson, M. Brechbiel, et al., J. Nucl. Med. 38 (1997) 200P.
[62] W.R. Harris, V.L. Pecoraro, Biochemistry 22 (1983) 292.
[63] C.L. Edwards, R.L. Hayes, J. Nucl. Med. 10 (1969) 103.
[64] S.W. Gunesekera, L.J. King, P.J. Lavender, Clin. Chim. Acta 39 (1972) 401.
[65] R.E. Weiner, Nucl. Med. Biol. 23 (1996) 745.
[66] M.A. Mintun, D.R. Dennis, M.J. Welch, C.J. Mathias, D.P. Schuster, J. Nucl. Med. 28 (1987) 1704.
[67] M.A. Green, M.J. Welch, C.J. Mathias, K.A. Fox, R.M. Knabb, J.C. Huffman, J. Nucl. Med. 26 (1985) 270.
[68] M.A. Green, J. Label. Compd. Radiopharm. 23 (1986) 1227.
[69] M.A. Green, C.J. Mathias, W.L. Neumann, P.E. Fanwick, M. Janick, E.A. Deutsch, J. Nucl. Med. 34 (1993) 228.
[70] B.W. Tsang, C.J. Mathias, M.A. Green, J. Nucl. Med. 34 (1993) 1127.
[71] B.W. Tsang, C.J. Mathias, P.E. Fanwick, M.A. Green, J. Med. Chem. 37 (1994) 4400.
[72] S. Liu, S.J. Rettig, C. Orvig, Inorg. Chem. 31 (1992) 5400.
[73] S. Liu, E. Wong, V. Karunaratne, S.J. Rettig, C. Orvig, Inorg. Chem. 32 (1993) 1756.
[74] Z. Zhang, D.M. Lyster, G.A. Webb, C. Orvig, Nucl. Med. Biol. 19 (1992) 327.
[75] H.F. Kung, B.L. Liu, D. Mankoff, M.P. Kung, J.J. Billings, L. Francesconi, et al., J. Nucl. Med. 31 (1990) 1635.
[76] L.C. Francesconi, B.L. Biu, J.J. Billings, P.J. Carroll, G. Graczyk, H.F. Kung J. Chem. Soc. Chem. Comm. (1991) 94.
[77] S.L. Madsen, M.J. Welch, R.J. Motekaitis, A.E. Martell, Nucl. Med. Biol. 19 (1992) 431.
[78] C.S. Cutler, D.E. Reichert, C.J. Anderson, M.C. Giron, R.J. Motekaitis, D.A. Quarless, et al., J. Label. Compd. Radiopharm. 40 (1997) 504.
[79] C.S. Cutler, M.C. Giron, D.E. Reichert, C.J. Anderson, S.A. Koch, D.A. Quarless, et al., J. Nucl. Med. 38 (1997) 125P.
[80] R.G. Pearson, J. Am. Chem. Soc. 85 (1963) 3533.
[81] A.E. Martell, R.D. Hancock, Metal Complexes in Aqueous Solutions, Plenum, New York, 1996.
[82] W.R. Harris, Y. Chen, K. Wein, Inorg. Chem. 33 (1994) 4991.

[83] D.A. Goodwin, R.A. Finston, L.G. Comombetti, J.E. Beaver, H.B. Hupf, J. Nucl. Med. 10 (1969) 337.
[84] W.W. Hunter Jr., H.W. DeCock, J. Nucl. Med. 10 (1969) 343.
[85] M.L. Thakur, Int. J. Appl. Radiat. Isot. 28 (1977) 183.
[86] M.J. Welch, T.J. Welch, Solution Chemistry of Carrier-Free Indium, Society of Nuclear Medicine, New York, 1975.
[87] M.J. Welch, S. Moerlein, Radiolabeled Compounds of Biomedical Interest Containing Radioisotopes of Gallium and Indium, vol. 140, American Chemical Society, Washington, DC, 1980.
[88] S.M. Moerlein, M.J. Welch, Int. J. Nucl. Med. Biol. 8 (1981) 277.
[89] C.J. Anderson, S.W. Schwarz, M.J. Welch, Indium, Marcel Dekker, Basel, 1994.
[90] D.A. Goodwin, C.H. Song, R. Finston, P. Matin, Radiology 108 (1973) 91.
[91] D.A. Goodwin, M.W. Sundberg, C.I. Diamanti, C.F. Meares, Radiopharmaceuticals, Society of Nuclear Medicine, New York, 1975.
[92] J.G. McAfee, M.L. Thakur, J. Nucl. Med. 18 (1976) 1022.
[93] R.M. Smith, A.E. Martell, Critical Stability Contants, vols. 1–6, Plennum, New York, 1989.
[94] M.A. Green, M.J. Welch, C.J. Mathias, P. Taylor, A.E. Martell, Nucl. Med. Biol. 12 (1985) 381.
[95] R.J. Motekaitis, Y. Sun, A.E. Martell, M.J. Welch, Inorg. Chem. 30 (1991) 2737.
[96] C.J. Mathias, Y. Sun, M.J. Welch, M.A. Green, J.A. Thomas, K.R. Wade, et al., Nucl. Med. Biol. 15 (1988) 69.
[97] R. Ma, R.J. Motekaitis, A.E. Martell, Inorg. Chim. Acta 224 (1994) 151.
[98] R.J. Motekaitis, Y. Sun, A.E. Martell, Inorg. Chim. Acta 159 (1989) 29.
[99] R.J. Motekaitis, A.E. Martell, M.J. Welch, Inorg. Chem. 29 (1990) 1463.
[100] C.J. Bannochie, A.E. Martell, J. Am. Chem. Soc. 111 (1989) 4735.
[101] C.J. Bannochie, A.E. Martell, Inorg. Chem. 30 (1991) 1385.
[102] S.L. Madsen, C.J. Bannochie, A.E. Martell, C.J. Mathias, M.J. Welch, J. Nucl. Med. 31 (1990) 1662.
[103] S.L. Madsen, C.J. Bannochie, M.J. Welch, C.J. Mathias, A.E. Martell, Nucl. Med. Biol. 18 (1991) 289.
[104] A.S. Craig, D. Parker, H. Adams, N.A. Bailey J. Chem. Soc. Chem. Commun. (1989) 1793.
[105] E.T. Clarke, A.E. Martell, Inorg. Chim. Acta 181 (1991) 273.
[106] E.T. Clarke, A.E. Martell, Inorg. Chim. Acta 190 (1992) 37.
[107] D.A. Moore, P.E. Fanwick, M.J. Welch, Inorg. Chem. 29 (1990) 672.
[108] R. Ma, M.J. Welch, J. Reibenspies, A.E. Martell, Inorg. Chim. Acta 236 (1995) 75.
[109] T.M. Jones-Wilson, R.J. Motekaitis, Y. Sun, C.J. Anderson, A.E. Martell, M.J. Welch, Nucl. Med. Biol. 22 (1995) 859.
[110] B.L. Liu, H.L. Kung, Y.T. Jin, L. Zhy, M. Meng, J. Nucl. Med. 30 (1989) 367.
[111] Y.Y. Zheng, S. Saluja, G.A. Yap, M. Blumenstein, A.L. Rheingold, L.C. Francesconi, Inorg. Chem. 35 (1996) 6656.
[112] C. Cotsyfakis, A.D. Varvarigou, M. Papadopoulos, S. Stathaki, C.I. Stassinopoulou, E. Chiotellis, Eur. J. Nucl. Med. 20 (1993) 302.
[113] C.S. John, S. Kinuya, G. Minear, R.K. Keast, C.H. Paik, Nucl. Med. Biol. 20 (1993) 217.
[114] C.J. Anderson, C.S. John, Y. Li, R.D. Hancock, T.J. McCarthy, A.E. Martell, et al., Nucl. Med. Biol. 22 (1995) 165.
[115] Y. Sun, R.J. Motekaitis, A.E. Martell, M.J. Welch, Inorg. Chim. Acta 228 (1995) 77.
[116] Y. Sun, R.J. Motekaitis, A.E. Martell, M.J. Welch, J. Coord. Chem. 36 (1995) 235.
[117] Y. Li, A.E. Martell, R.D. Hancock, J.H. Reibenspies, C.J. Anderson, M.J. Welch, Inorg. Chem. 35 (1996) 404.
[118] Y. Sun, C.J. Anderson, T.S. Pajeau, D.E. Reichert, R.D. Hancock, R.J. Motekaitis, et al., J. Med. Chem. 39 (1996) 458.
[119] L.A. Bass, D.W. McCarthy, L.A. Jones, P.D. Cutler, R.E. Shefer, R.E. Klinkowstein, et al., J. Label. Compd. Radiopharms. 40 (1997) 325.
[120] D.W. McCarthy, R.E. Shefer, R.E. Klinkowstein, L.A. Bass, W.H. Margeneau, C.S. Cutler, et al., Nucl. Med. Biol. 24 (1997) 35.
[121] P.J. Blower, J.S. Lewis, J. Zweit, Nucl. Med. Biol. 23 (1996) 957.

[122] R.J. Motekaitis, B.E. Rogers, D.E. Reichert, A.E. Martell, M.J. Welch, Inorg. Chem. 35 (1996) 3821.
[123] B.E. Rogers, C.J. Anderson, J.M. Connett, L.W. Guo, W.B. Edwards, E.L.C. Sherman, et al., Bioconjugate Chem. 7 (1996) 511.
[124] J.S. Lewis, J. Zweit, J.L.J. Dearling, B.C. Rooney, P.J. Blower, Chem. Commun. (1996) 1093.
[125] J.S. Lewis, J.L.J. Dearling, B.C. Rooney, H. Coley, L. Kelland, J. Zweit, et al., J. Nucl. Med. 41 (1997) 9P.
[126] Y. Fujibayashi, H. Taniuchi, Y. Yonekura, H. Ohtani, J. Konishi, A. Yokoyama, J. Nucl. Med. 38 (1997) 115.
[127] H. Taniuchi, Y. Fujibayashi, Y. Yonekura, J. Konishi, A. Yokoyama, J. Nucl. Med. 38 (1997) 1130.
[128] J.K. Lim, C.J. Mathias, M.A. Green, J. Med. Chem. 40 (1997) 132.
[129] C.E. Housecroft, Coord. Chem. Rev. 146 (1995) 155.
[130] H. Herzog, F. Rosch, G. Stocklin, C. Lueders, S.M. Qaim, L.E. Feinendegen, J. Nucl. Med. 34 (1993) 2222.
[131] H.-J. Wester, J. Brockmann, F. Rosch, W. Wutz, H. Herzog, P. Smith-Jones, et al., Nucl. Med. Biol. 24 (1997) 275.
[132] H. Herzog, F. Rosch, J. Brockmann, H. Muhlensiepen, M. Kohle, B. Stolz, et al., J. Nucl. Med. 38 (1997) 60P.
[133] D.J. Hnatowich, M. Chinol, D.A. Siebecker, M. Gionet, T. Griffin, P.W. Doherty, et al., J. Nucl. Med. 29 (1988) 1428.
[134] S.V. Deshpande, S.J. DeNardo, D.L. Kukis, M.K. Moi, M.J. McCall, G.L. DeNardo, et al., J. Nucl. Med. 31 (1990) 473.
[135] C.F. Meares, Nucl. Med. Biol. 13 (1986) 311.
[136] R. Subramanian, C.F. Meares, in: D.M. Goldenberg (Ed.), Cancer Imaging with Radiolabelled Antibodies, Kluwer Academic Publishers, Boston, 1990, p. 183.
[137] R.S. Wu, in: D.M. Goldenberg (Ed.), Cancer Imaging with Radiolabelled Antibodies, Kluwer Academic Publishers, Boston, 1990, p. 215.
[138] D. Parker, Chem. Soc. Rev. 19 (1990) 271.
[139] L.I. Delmon-Moingeon, A. Mahmood, A. Davison, A.G. Jones, J. Nucl. Med. Biol. 35 (1991) 47.
[140] O.A. Gansow, Nucl. Med. Biol. 18 (1991) 369.
[141] P.A. Schubiger, R. Alberto, A. Smith, Bioconjugate Chem. 7 (1996) 165.
[142] M.W. Sundberg, C.F. Meares, D.A. Goodwin, J. Med. Chem. 17 (1974) 1304.
[143] C.F. Meares, D.A. Goodwin, C.S.-H. Leung, A.Y. Girgis, D.J. Silvester, A.D. Nunn, et al., Proc. Natl. Acad. Sci. USA 73 (1976) 3803.
[144] G.E. Krejcarek, K.L. Tucker, Biochem. Biophys. Res. Commun. 77 (1977) 581.
[145] D.J. Hnatowich, W.W. Layne, R.L. Childs, Science 220 (1983) 613.
[146] D.J. Hnatowich, in: S.P. Fricker (Ed.), The In Vivo Use of Metallic Radioisotopes in Cancer Detection and Imaging, Chapman and Hall, London, 1994, p. 215.
[147] B.A. Rhodes, Nucl. Med. Biol. 18 (1991) 667.
[148] W.C. Eckelman, J. Steigman, Nucl. Med. Biol. 18 (1991) 3.
[149] G.L. Griffiths, D.M. Goldenberg, A.L. Jones, H.J. Hansen, Bioconjugate Chem. 3 (1992) 91.
[150] P.O. Zamora, S. Guhlke, H. Bender, D. Diekmann, B.A. Rhodes, H.-J. Biersack, et al., Int. J. Cancer 65 (1996) 214.
[151] M.L. Thakur, H.R. Kolan, E. John, S. Rifat, J. Li, A. Rux, et al., Int. J. Oncol. 9 (1996) 445.
[152] M.L. Thakur, H. Kolan, J. Li, R. Wiaderkiewicz, V.R. Pallela, R. Duggaraju, et al., Nucl. Med. Biol. 24 (1997) 105.
[153] J. Quinomones, G. Mizejewski, W.M. Beierwaltes, J. Nucl. Med. 12 (1971) 69.
[154] F.J. Primus, R.H. Wang, D.M. Goldenberg, H.J. Hansen, Cancer Res. 33 (1973) 2977.
[155] D.M. Goldenberg, D.F. Present, F.J. Primus, H.J. Hansen, Cancer Res. 34 (1974) 1.
[156] R. Guillemin, Science 202 (1978) 390.
[157] S. Reichlin, N. Eng. J. Med. 309 (1983) 1495.
[158] S. Reichlin, N. Engl. J. Med. 309 (1983) 1556.
[159] J.C. Reubi, L.K. Kvols, E.P. Krenning, S.W.J. Lamberts, Metabolism 39 (1990) 78.

[160] W. Bauer, U. Briner, W. Doepfner, R. Haller, R. Huguenin, P. Marbach, et al., Life Sci. 31 (1982) 1133.
[161] W.H. Bakker, R. Albert, C. Bruns, W.A.P. Breeman, L.J. Hofland, P. Marbach, et al., Life Sci. 49 (1991) 1583.
[162] W.H. Bakker, E.P. Krenning, W.A. Breeman, P.P.M. Kooij, J.C. Reubi, J.W. Koper, et al., J. Nucl. Med. 32 (1991) 1184.
[163] E.P. Krenning, W.H. Bakker, P.P.M. Kooij, W.A.P. Breeman, H.Y. Oei, M. de Jong, et al., J. Nucl. Med. 33 (1992) 652.
[164] P.M. Smith-Jones, B. Stolz, C. Bruns, R. Albert, H.W. Reist, R. Fridrich, et al., J. Nucl. Med. 35 (1994) 317.
[165] B. Stolz, P.M. Smith-Jones, R. Albert, H. Reist, H. Macke, C. Bruns, Horm. Metab. Res. 26 (1994) 452.
[166] G. Anderegg, F. L'Eplattenier, G. Schwarzenbach, Helv. Chim. Acta 46 (1963) 1400.
[167] S. Moeschlin, U. Scnider, N. Engl. J. Med. 269 (1963) 57.
[168] A. Yokoyama, Y. Ohmono, K. Horiuchi, H. Saji, H. Tanaka, K. Yamamoto, et al., J. Nucl. Med. 23 (1982) 909.
[169] C.J. Anderson, T.S. Pajeau, W.B. Edwards, E.L.C. Sherman, B.E. Rogers, M.J. Welch, J. Nucl. Med. 36 (1995) 2315.
[170] F. Dehdashti, C.J. Anderson, D.D. Trask, L.A. Bass, S.W. Schwarz, P.D. Cutler, et al., J. Nucl. Med. 38 (1997) 103P.
[171] P.M. Smith-Jones, B. Stolz, R. Albert, G. Ruser, H. Mäcke, U. Briner, et al., J. Label. Compd. Radiopharm. 37 (1995) 499.
[172] M. de Jong, W.H. Bakker, E.P. Krenning, W.A.P. Breeman, M.E. van der Pluijm, B.F. Bernard, et al., Eur. J. Nucl. Med. 24 (1997) 368.
[173] B. Stolz, P. Smith-Jones, R. Albert, L. Tolcsvai, U. Briner, G. Ruser, et al., Digestion 57 (1996) 17.
[174] H.R. Kolan, M.L. Thakur, R. Wiaderkiewicz, J. Li, R. Duggaraju, J. Label. Compd. Radiopharm. 37 (1995) 490.
[175] J.M. Varum, M. Thakur, A.V. Schally, S. Jansen, K.H. Mayo, J. Biol. Chem. 269 (1994) 12583.
[176] P.O. Zamora, M.J. Marek, F.F.J. Knapp, Appl. Radiat. Isot. 48 (1997) 305.
[177] D.A. Pearson, J. Lister-James, W.J. McBride, D.M. Wilson, L.J. Martel, E.R. Civitello, et al., J. Med. Chem. 39 (1996) 1361.
[178] S. Vallabhajosula, B.R. Moyer, J. Lister-James, B.J. McBride, H. Lipszyc, H. Lee, et al., J. Nucl. Med. 37 (1996) 1016.
[179] C.J. Palestro, R. Bitton, M.B. Tomas, D. Myssiorek, K.K. Bhargava, Y.M. Baran, J. Nucl. Med. 38 (1997) 236P.
[180] S. Wang, R.J. Lee, C.J. Mathias, M.A. Green, P.S. Low, Bioconjugate Chem. 7 (1996) 56.
[181] C.J. Mathias, S. Wang, R.J. Lee, D.J. Waters, P.S. Low, M.A. Green, J. Nucl. Med. 37 (1996) 1003.
[182] C.J. Mathias, D.P. Hubers, D.P. Trump, S. Wang, J. Luo, D.J. Waters, et al., J. Nucl. Med. 38 (1997) 87P.
[183] C.J. Mathias, S. Wang, D.J. Waters, J.J. Turek, P.S. Low, M.A. Green, J. Nucl. Med. 38 (1997) 133P.
[184] D.M. Goldenberg, Cancer Imaging and Therapy with Radiolabeled Antibodies, Plenum Press, New York, 1991.
[185] T.A. Waldmann, Science 252 (1991) 1657.
[186] T.J. McKearn, Cancer 71 (1993) 4302.
[187] K. Liewendahl, S. Pyrhonen, Acta Oncol. 32 (1993) 717.
[188] A.R. Fritzberg, P.L. Beaumeier, B.J. Bottino, J.M. Reno, J. Control. Release 28 (1994) 167.
[189] A.B. Delaloye, B. Delaloye, Eur. J. Nucl. Med. 22 (1995) 571.
[190] T. Stigbrand, A. Ullen, P. Sandstrom, H. Mirzaie-Joniani, B. Sundstrom, B. Nilsson, et al., Acta Oncol. 35 (1996) 259.
[191] H.A. Nabi, Clin. Immunother. 6 (1996) 200.
[192] L.S. Zuckier, G.L. Denardo, Sem. Nucl. Med. 27 (1997) 10.

[193] J.A. Katzenellenbogen, K.D. McElvany, S.G. Senderoff, K.E. Carlson, S.W. Landvatter, M.J. Welch, J. Nucl. Med. 22 (1981) 42.
[194] R.N. Hanson, L.A. Franke, J. Nucl. Med. 25 (1984) 998.
[195] D.O. Kiesewetter, M.R. Kilbourn, S.W. Landvatter, D.F. Heiman, J.A. Katzenellenbogen, M.J. Welch, J. Nucl. Med. 25 (1984) 1212.
[196] J.P. DiZio, R. Fiaschi, A. Davison, A.G. Jones, J.A. Katzenellenbogen, Bioconjugate Chem. 2 (1991) 353.
[197] J.P. DiZio, C.J. Anderson, A. Davison, G.J. Ehrhardt, K.E. Carlson, M.J. Welch, et al., J. Nucl. Med. 33 (1992) 558.
[198] J.P. O'Neil, K.E. Carlson, C.J. Anderson, M.J. Welch, J.A. Katzenellenbogen, Bioconjugate Chem. 5 (1994) 182.
[199] S. Top, H. El Hafa, A. Vessieres, J. Quivy, J. Vaissermann, D.W. Hughes, et al., J. Am. Chem. Soc. 117 (1995) 8372.
[200] D.Y. Chi, J.A. Katzenellenbogen, J. Am. Chem. Soc. 115 (1993) 7045.
[201] D.Y. Chi, J.P. O'Neil, C.J. Anderson, M.J. Welch, J.A. Katzenellenbogen, Bioconjugate Chem. 37 (1994) 928.
[202] R.K. Rom, D.Y. Chi, J.A. Katzenellenbogen, J. Org. Chem. 61 (1996) 2624.
[203] C.S. John, B.B. Lim, B.C. Beyer, B.J. Vilner, W.D. Bowen, Bioconjugate Chem. 8 (1997) 304.
[204] M.F. Giblin, S.S. Jurisson, T.P. Quinn, Bioconjugate Chem. 8 (1997) 347.
[205] M.J. Kaufman, B.K. Madras, Synapse 9 (1991) 43.
[206] B.K. Madras, A.G. Jones, A. Mahmood, R.E. Zimmerman, B. Garada, B.L. Holman, et al., Synapse 22 (1996) 239.
[207] P.C. Meltzer, B.K. Madras, Eur. J. Nucl. Med. 24 (1997) 462.
[208] S. Meegalla, K. Plossl, M.P. Kung, S. Chumpradit, D.A. Stevenson, D. Frederick, et al., Bioconjugate Chem. 7 (1996) 421.
[209] M.P. Kung, D.A. Stevenson, K. Plossl, S.K. Meegalla, A. Beckwith, W.D. Essman, et al., Eur. J. Nucl. Med. 24 (1997) 372.
[210] A. Davison, A.G. Jones, C. Orvig, M. Sohn, Inorg. Chem. 20 (1980) 1629.
[211] D.J. Canney, J. Billings, L.C. Francesconi, Y.-Z. Guo, B.S. Haggerty, A.L. Rheingold, et al., J. Med. Chem. 36 (1993) 1032.
[212] L.C. Francesconi, Y.Y. Yang, M.-P. Kung, X.X. Zhang, J.J. Billings, Y.-Z. Guo, et al., J. Med. Chem. 37 (1994) 3282.
[213] A.R. Fritzberg, P.G. Abrams, P.L. Beaumier, S. Kasina, A.C. Morgan, T.N. Rao, et al., Proc. Natl. Acad. Sci. USA 85 (1988) 4025.
[214] S.K. Meegalla, K. Plossl, M.P. Kung, S. Chumpradit, D.A. Stevenson, S.A. Kushner, et al., J. Med. Chem. 40 (1997) 9.
[215] H.F. Kung, H.J. Kim, M.P. Kung, S.K. Meegalla, K. Plossl, H.K. Lee, Eur. J. Nucl. Med. 23 (1996) 1527.
[216] A.J. Fischman, M.C. Pike, D. Kroon, A.J. Fucello, D. Rexinger, C. ten Kate, et al., J. Nucl. Med. 32 (1991) 483.
[217] M.J. Abrams, S.K. Larsen, J. Zubieta, Inorg. Chim. Acta 173 (1990) 133.
[218] J.A. Abrams, M. Juweid, C.I. tenKate, D.A. Schwartz, M.M. Hauser, F.E. Gaul, et al., J. Nucl. Med. 31 (1990) 2022.
[219] J.W. Babich, H. Solomon, M.C. Pike, D. Kroon, W. Graham, M.J. Abrams, et al., J. Nucl. Med. 34 (1993) 1964.
[220] J.W. Babich, W. Graham, S.A. Barrow, S.C. Dragotakes, R.G. Tompkins, R.H. Rubin, et al., J. Nucl. Med. 34 (1993) 2176.
[221] A.J. Fischman, J.W. Babich, S.A. Barrow, W. Graham, E. Carter, R.G. Tompkins, et al., J. Trauma 38 (1995) 223.
[222] J.W. Babich, A.J. Fischman, Nucl. Med. Biol. 22 (1995) 25.
[223] C.J. van der Laken, O.C. Boerman, W.J.G. Oyen, M.T.P. van de Ven, D.S. Edwards, J.A. Barrett, J.W.M. van der Meer, F.H.M. Corstens, J. Nucl. Med. 38 (1997) 1310.
[224] J.W. Babich, R.G. Tompkins, W. Graham, S.A. Barrow, A.J. Fischman, J. Nucl. Med. 38 (1997) 1316.

[225] S. Vallabhajosula, J. Nucl. Med 38 (1997) 1322.
[226] D. Som, Z.H. Oster, J. Nucl. Med. 35 (1994) 202.
[227] P. deFaucal, P. Peltier, B. Planchon, J. Nucl. Med. 32 (1991) 785.
[228] G.J. Wang, Z.H. Oster, P. Som, P.O. Zamora, Int. J. Radiat. Appl. Instrum.-Part B, Nucl. Med. Biol. 18 (1991) 275.
[229] L.C. Knight, R. Radcliffe, A.H. Maurer, J.D. Rodwell, V.L. Alvarez, J. Nucl. Med. 35 (1994) 282.
[230] L.C. Knight, A.H. Maurer, I.A. Ammar, L.A. Epps, R.T. Dean, K.Y. Pak, et al., Radiology 173 (1989) 163.
[231] L.C. Knight, M.J. Abrams, D.A. Schwartz, M.M. Hauser, M. Kollman, F.E. Gaul, et al., J. Nucl. Med. 33 (1992) 710.
[232] F.T. Lee, L.J. Milner, G.R. Boniface, G.J. Bautovich, A.R. Weedon, P.G. Bundesen, et al., Immun. Cell Biol. 70 (1992) 173.
[233] F.T. Lee, G.R. Boniface, R.M. Lambrecht, D.B. Rylatt, P.G. Bundesen, Immun. Cell Biol. 71 (1993) 117.
[234] P. Muto, S. Lastoria, P. Varrella, E. Vergara, M. Salvatore, G. Morgano, et al., J. Nucl. Med. 36 (1995) 1384.
[235] J. Lister-James, L.C. Knight, A.H. Maurer, L.R. Bush, B.R. Moyer, R.T. Dean, J. Nucl. Med. 37 (1996) 775.
[236] J. Lister-James, S. Vallabhajosula, B.R. Moyer, D.A. Pearson, B.J. McBride, M.A. De Rosch, et al., J. Nucl. Med. 38 (1997) 105.
[237] D.A. Pearson, J. Lister, W.J. McBride, D.M. Wilson, L.J. Martel, E.R. Civitello, et al., J. Med. Chem. 39 (1996) 1372.
[238] J.A. Barrett, D.J. Damphousse, S.J. Heminway, S. Liu, D.S. Edwards, R.J. Looby, et al., Bioconjugate Chem. 7 (1996) 203.
[239] S. Liu, D.S. Edwards, R.J. Looby, M.J. Poirier, M. Rajopadhye, J.P. Bourque, et al., Bioconjugate Chem. 7 (1996) 196.
[240] M. Rajopadhye, D.S. Edwards, J.P. Bourque, T.R. Carroll, Bioorg. Med. Chem. Lett. 6 (1996) 1737.
[241] M. Rajopadhye, T.D. Harris, K. Yu, D. Glowacka, P.R. Damphousse, J.A. Barrett, et al., Bioorg. Med. Chem. Lett. 7 (1997) 955.
[242] S. Liu, D.S. Edwards, R.J. Looby, A.R. Harris, M.J. Poirier, J.A. Barrett, et al., Bioconjugate Chem. 7 (1996) 63.
[243] J.A. Barrett, A.C. Crocker, D.J. Damphousse, S.J. Heminway, S. Liu, D.S. Edwards, et al., Bioconjugate Chem. 8 (1997) 155.
[244] D.S. Edwards, S. Liu, J.A. Barrett, A.R. Harris, R.J. Looby, M.C. Ziegler, et al., Bioconjugate Chem. 8 (1997) 146.
[245] R.B. Lauffer, Chem. Rev. 87 (1987) 901.
[246] G.L. Wolf, Radiology 172 (1989) 709.
[247] S.H. Koenig, Acta Radiol. Suppl. 374 (1990) 17.
[248] R.B. Lauffer, Magn. Reson. Quart. 6 (1990) 65.
[249] D.L. White, Magn. Reson. Med. 22 (1991) 309.
[250] G.M. Bydder, Top. Magn. Reson. Imaging 3 (1991) 74.
[251] M.F. Tweedle, J. Alloys Compd. 180 (1992) 317.
[252] C.A. Chang, Invest. Radiol. 28 (1993) 21.
[253] E.C. Unger, D.K. Shen, T.A. Fritz, J. Magn. Reson. Imaging 3 (1993) 195.
[254] S.M. Rocklage, A.D. Watson, J. Magn. Reson. Imaging 3 (1993) 167.
[255] G. Schuhmann-Giampieri, Invest. Radiol. 28 (1993) 753.
[256] R.E. Hendrick, E.M. Haacke, J. Magn. Reson. Imaging 3 (1993) 137.
[257] R. Mathur-De Vre, M. Lemort, Br. J. Radiol. 68 (1995) 225.
[258] H. Gupta, R. Weissleder, Magn. Reson. Imaging Clin. N. Am. 4 (1996) 171.
[259] D. Parker, J.A.G. Williams, J. Chem. Soc., Dalton Trans. (1996) 3613.
[260] S. Aime, M. Botta, M. Fasano, S. Paoletti, P.L. Anelli, F. Uggeri, et al., Inorg. Chem. 33 (1994) 4707.
[261] V.W.-W. Yam, K.K.-W. Lo, Coord. Chem. Rev. 131 (1998).

[262] N. Hocine, J.P. Berry, H. Jaafoura, F. Escaig, R. Masse, P. Galle, Cell. Mol. Biol. 41 (1995) 271.
[263] W.P. Cacheris, S.C. Quay, S.M. Rocklage, Magn. Reson. Imaging 8 (1990) 467.
[264] M.F. Tweedle, J.J. Hagan, K. Kumar, S. Mantha, C.A. Chang, Magn. Reson. Imaging 9 (1991) 409.
[265] M.F. Tweedle, P. Wedeking, K. Kumar, Invest. Radiol. 30 (1995) 372.
[266] J.R. Duncan, F.N. Franano, W.B. Edwards, M.J. Welch, Invest. Radiol. 29 (1994) 58.
[267] K. Micskei, D.H. Powell, L. Helm, E. Brücher, A.E. Merbach, Magn. Reson. Chem. 31 (1993) 1011.
[268] D. Pubanz, G. González, D.H. Powell, A.E. Merbach, Inorg. Chem. 34 (1995) 4447.
[269] X. Zhang, C.A. Chang, H.G. Brittain, J.M. Garrison, J. Telser, M.F. Tweedle, Inorg. Chem. 31 (1992) 5597.
[270] C.A. Chang, H.G. Brittain, J. Telser, M.F. Tweedle, Inorg. Chem. 29 (1990) 4468.
[271] S. Aime, P.L. Anelli, M. Botta, F. Fedeli, M. Grandi, P. Paoli, et al., Inorg. Chem. 31 (1992) 2422.
[272] F. Uggeri, S. Aime, P.L. Anelli, M. Botta, M. Brochetta, C. de Haën, et al., Inorg. Chem. 34 (1995) 633.
[273] H.J. Weinmann, R.C. Brasch, W.R. Press, G.E. Wesbey, Am. J. Roentgenol. 142 (1984) 619.
[274] H. Gries, H. Miklautz, Phys. Chem. Phys. Med. NMR 16 (1984) 105.
[275] R.C. Brasch, H.J. Weinmann, G.E. Wesbey, Am. J. Roentgenol. 142 (1984) 625.
[276] P. Wedeking, M. Tweedle, Nucl. Med. Biol. 15 (1988) 395.
[277] M. Laniado, H.J. Weinmann, W. Schorner, R. Felix, U. Speck, Phys. Chem. Phys. Med. NMR 16 (1984) 157.
[278] H.J. Weinmann, M. Laniado, W. Mutzel, Phys. Chem. Phys. Med. NMR 16 (1984) 167.
[279] D.H. Carr, J. Brown, G.M. Bydder, H.J. Weinmann, U. Speck, D.J. Thomas, et al., Lancet 1 (1984) 484.
[280] D.H. Carr, J. Brown, G.M. Bydder, R.E. Steiner, H.J. Weinmann, U. Speck, et al., Am. J. Roentgenol. 143 (1984) 215.
[281] S.C. Quay, Diamide–DTPA-Paramagnetic Contrast Agents for MR Imaging, Salutar, USA, 1987.
[282] M.S. Konigs, W.C. Dow, D.B. Love, K.N. Raymond, S.C. Quay, S.M. Rocklage, Inorg. Chem. 29 (1990) 1488.
[283] E.S. Harpur, D. Worah, P.A. Hals, E. Holtz, K. Furuhama, H. Nomura, Invest. Radiol. 28 (1993) 28.
[284] M. Van Wagoner, D. Worah, Invest. Radiol. 28 (1993) 41.
[285] H.J. Weinmann, G. Schuhmann-Giampieri, H. Schmitt-Willich, H. Vogler, T. Frenzel, H. Gries, Magn. Reson. Med. 22 (1991) 233.
[286] G. Schuhmann-Giampieri, H. Schmitt-Willich, W.R. Press, C. Negishi, H.J. Weinmann, U. Speck, Radiology 183 (1992) 59.
[287] A. Mühler, R.P.J. Oude Elferink, H.-J. Weinmann, MAGMA 1993 (1993) 134.
[288] A. Muhler, I. Heinzelmann, H.J. Weinmann, Invest. Radiol. 29 (1994) 213.
[289] B. Hamm, T. Staks, A. Muhler, M. Bollow, M. Taupitz, T. Frenzel, et al., Radiology 195 (1995) 785.
[290] G. Benness, M. Khangure, I. Morris, A. Warwick, P. Burrows, H. Vogler, et al., Invest. Radiol. 31 (1996) 211.
[291] M. Bollow, M. Taupitz, B. Hamm, T. Staks, K.J. Wolf, H.J. Weinmann, Eur. Radiol. 7 (1997) 126.
[292] G. Vittadini, E. Felder, P. Tirone, V. Lorusso, Invest. Radiol. 23 (1988) 246.
[293] P. Pavone, G. Patrizio, C. Buoni, E. Tettamanti, R. Passariello, C. Musu, et al., Radiology 176 (1990) 61.
[294] T.J. Vogl, W. Pegios, C. McMahon, J. Balzer, J. Waitzinger, G. Pirovano, et al., Am. J. Roentgenol. 158 (1992) 887.
[295] R. Caudana, G. Morana, G.P. Pirovano, N. Nicoli, A. Portuese, A. Spinazzi, et al., Radiology 199 (1996) 513.
[296] W. Schima, J. Petersein, P.F. Hahn, M. Harisinghani, E. Halpern, S. Saini, J. Magn. Reson. Imaging 7 (1997) 130.

[297] M. Magerstadt, O.A. Gansow, M.W. Brechbiel, D. Colcher, L. Baltzer, R.H. Knop, et al., Magn. Reson. Med. 3 (1986) 808.
[298] R.H. Knop, J.A. Frank, A.J. Dwyer, M.E. Girton, M. Naegele, M. Schrader, et al., J. Comp. Assist. Tomogr. 11 (1987) 35.
[299] J.C. Bousquet, S. Saini, D.D. Stark, P.F. Hahn, M. Nigam, J. Wittenberg, et al., Radiology 166 (1988) 693.
[300] J.-P. Dubost, J.-M. Leger, M.-H. Langlois, D. Meyer, M. Schaefer, C. R. Acad. Sci., Ser. 2 312 (1991) 349.
[301] C.A. Chang, L.C. Francesconi, M.F. Malley, K. Kumar, J.Z. Gougoutas, M.F. Tweedle, et al., Inorg. Chem. 32 (1993) 3501.
[302] M.M. Le Mignon, C. Chambon, S. Warrington, R. Davies, B. Bonnemain, Invest. Radiol. 25 (1990) 933.
[303] M. Oudkerk, P.E. Sijens, E.J. Van Beek, T.J. Kuijpers, Invest. Radiol. 30 (1995) 75.
[304] M.F. Tweedle, S.M. Eaton, W.C. Eckelman, G.T. Gaughan, J.J. Hagan, P.W. Wedeking, et al., Invest. Radiol. 23 (1988) 236.
[305] D.D. Dischino, E.J. Delaney, J.E. Emswiler, G.T. Gaughan, J.S. Prasad, S.K. Srivastava, et al., Inorg. Chem. 30 (1991) 1265.
[306] V.M. Runge, D.M. Kaufman, M.L. Wood, L.S. Adelman, S. Jacobson, Int. J. Radiat. Appl. Instrum.-Part B, Nucl. Med. Biol. 16 (1989) 561.
[307] M.F. Tweedle, Invest. Radiol. 27 (1992) 2.
[308] K. Kumar, C.A. Chang, L.C. Francesconi, D.D. Dischino, M.F. Malley, J.Z. Gougoutas, et al., Inorg. Chem. 33 (1994) 3567.
[309] R.A. Soltys, Invest. Radiol. 27 (1992) 7.
[310] D. DeSimone, M. Morris, C. Rhoda, T. Lucas, J. Zielonka, A. Olukotun, et al., Invest. Radiol. 26 (1991) 212.
[311] S.J. McLachlan, S. Eaton, D.N. De Simone, Invest. Radiol. 27 (1992) 12.
[312] M.J. Carvlin, D.N. De Simone, M.J. Meeks, Invest. Radiol. 27 (1992) 16.
[313] V.M. Runge, W.G. Bradley, M.N. Brant-Zawadzki, M.J. Carvlin, D.N. DeSimone, B.L. Dean, et al., Radiology 181 (1991) 701.
[314] M. Seiderer, Invest. Radiol. 27 (1992) 33.
[315] A.Y. Olukotun, J.R. Parker, M.J. Meeks, M.A. Lucas, D.R. Fowler, T.R. Lucas, J. Magn. Reson. Imaging 5 (1995) 17.
[316] M.F. Tweedle, G.T. Gaughan, J. Hagan, P.W. Wedeking, P. Sibley, L.J. Wilson, et al., Int. J. Radiat. Appl. Instrum.-Part B, Nucl. Med. Biol. 15 (1988) 31.
[317] V.M. Runge, T.H. Pels Rijcken, A. Davidoff, J.W. Wells, D.D. Stark, J. Magn. Reson. Imaging 4 (1994) 281.
[318] S.J. McLachlan, M.R. Morris, M.A. Lucas, R.A. Fisco, M.N. Eakins, D.R. Fowler, et al., J. Magn. Reson. Imaging 4 (1994) 301.
[319] D. Pouliquen, H. Perroud, F. Calza, P. Jallet, J.J. Le Jeune, Magn. Reson. Med. 24 (1992) 75.
[320] R.B. Lauffer, W.L. Greif, D.D. Stark, A.C. Vincent, S. Saini, V.J. Wedeen, et al., J. Comp. Assist. Tomogr. 9 (1985) 431.
[321] F. Shtern, L. Garrido, C. Compton, J.K. Swiniarski, R.B. Lauffer, T.J. Brady, Radiology 178 (1991) 83.
[322] H. Macapinlac, B. Engelstad, E. Ramos, D. White, T. Johnson, M. Moseley, Magn. Reson. Imaging 1 (1987) 97.
[323] N.A. Bailey, D. Cummins, E.D. McKenzie, Inorg. Chim. Acta 50 (1981) 111.
[324] R.B. Lauffer, A.C. Vincent, S. Padmanabhan, A. Villringer, S. Saini, D.R. Elmaleh, et al., Magn. Reson. Med. 4 (1987) 582.
[325] B.G. Jenkins, E. Armstrong, R.B. Lauffer, Magn. Reson. Med. 17 (1991) 164.
[326] S.M. Rocklage, W.P. Cacheris, S.C. Quay, F.E. Hahn, K.N. Raymond, Inorg. Chem. 28 (1989) 477.
[327] S.M. Rocklage, M. Vanwagoner, in: J.T. Ferrucci, D.D. Stark (Eds.), Hepatobiliary Contrast Agents: An Overview of the Development of Manganese Dipyridoxyl Diphosphate (Mn–DPDP), Andover Medical Publishers, Boston, 1990, p. 374.

[328] O.H. Pomeroy, M. Wendland, S. Wagner, N. Derugin, W.W. Holt, S.M. Rocklage, et al., Invest. Radiol. 24 (1989) 531.
[329] M.E. Bernardino, S.W. Young, J.K. Lee, J. Weinreb, Invest. Radiol. 26 (1991) 148.
[330] E. Rummeny, C. Ehrenheim, H.B. Gehl, B. Hamm, M. Laniado, K.P. Lodemann, et al., Invest. Radiol. 26 (1991) 142.
[331] N.M. Rofsky, J.C. Weinreb, Magn. Reson. Quart. 8 (1992) 156.
[332] R.C. Brasch, Magn. Reson. Med. 22 (1991) 282.
[333] M.W. Brechbiel, O.A. Gansow, Bioconjugate Chem. 2 (1991) 187.
[334] E.C. Wiener, M.W. Brechbiel, H. Brothers, R.L. Magin, O.A. Gansow, D.A. Tomalia, et al., Magn. Reson. Med. 31 (1994) 1.
[335] W.C. Eckelman, M. Tweedle, M.J. Welch, in: S. Srivastava (Ed.), NMR Enhancement with Gadolinium-Labeled Antibodies, vol. 152, Plenum Publishing, New York, 1988, p. 571.
[336] M.J. Welch, Acta Radiol. Suppl. 374 (1990) 129.
[337] E.C. Unger, W.G. Totty, D.M. Neufeld, F.L. Otsuka, W.A. Murphy, M.S. Welch, et al., Invest. Radiol. 20 (1985) 693.
[338] P.F. Sieving, A.D. Watson, S.M. Rocklage, Bioconjugate Chem. 1 (1990) 65.
[339] A. Muhler, J. Platzek, B. Raduchel, T. Frenzel, H.J. Weinmann, J. Magn. Reson. Imaging 5 (1995) 7.
[340] Table of Isotopes, 7th edn., Vol. 7, Wiley, New York, 1978.
[341] M.R. Zaman, S.M. Qaim, Radiochim. Acta 75 (1996) 59.
[342] C. Loc'h, B. Mazièré, D. Comar, J. Nucl. Med. 21 (1979) 171.
[343] F. Rösch, S.M. Qaim, G. Stöcklin, Appl. Radiat. Isot. 44 (1993) 677.
[344] R.J. Nickles, A.D. Nunn, C.K. Stone, B.T. Christian, J. Nucl. Med. 34 (1993) 1058.
[345] E.T. Clarke, A.E. Martell, Inorg. Chim. Acta 186 (1991) 103.
[346] A.E. Martell, R.J. Motekaitis, M.J. Welch, J. Chem. Soc. Chem. Commun. (1990) 1748.
[347] R.J. Motekaitis, Y. Sun, A.E. Martell, Inorg. Chim. Acta 198-200 (1992) 421.
[348] NIST Critical Stability Constants of Metal Complexes Database No. 46, US Department of Commerce, Washington DC, 1993.
[349] M. Schaeffer, D. Meyer, S. Beaute, D. Doucet, Magn. Reson. Med. 22 (1991) 238.

Glossary

(4,6-MeO$_2$sal)$_2$BAPEN:	bis(4,6-dimethoxysalicylaldimino)-*N*,*N*′-bis(3-aminopropyl)ethylenediamine
(ROsal)$_3$tame:	1,1,1-tris-(alkoxysalicylaldiminomethyl)ethane
(5-MeOsal)$_3$tame:	1,1,1-tris-(5-methoxysalicylaldiminomethyl)ethane
4SS:	*N*,*N*′-bis(2,2-dimethyl-2-mercaptoethyl)ethylenediamine
5SS1:	carboxy-*N*,*N*′-bis(2,2-dimethyl-2-mercaptoethyl)ethylenediamine
6SS:	*N*,*N*′-bis(2,2,-dimethyl-2-mercaptoethyl)ethylenediamine-*N*,*N*-diacetic acid
ATSM:	diacetyl-bis(N^4-methylthiosemicarbazone)
BAT:	6-[*p*-(bromoacetamido)benzyl]-1,4-8-11-tetraazacyclotetradecane-1,4,8,11-tetracetic acid
BAT–TECH:	tetraethyl-cyclohexyl bis-aminoethanethiol
BFC:	bifunctional chelator
BMS-181321:	oxo((3,3,9,9-tetramethyl-1-(2-nitro-1H-imidazol-1-yl)-4,8-diazaundecane-2,10-dione dioximato)(3-)-*N*,*N*′,*N*″,*N*‴)technetium(V)

BOPTA:	4-carboxy-5,8,11-tris(carboxymethyl)-1-phenyl-2-oxa-5,8,11-triazatridecan-13-oic acid:benic acid
CPTA:	4-[(1,4,8,11-tetraazacyclotetradec-1-yl)methyl]benzoic acid
DATs:	Dopamine transporters
DF:	desferrioxamine-B
DMPE:	1,2-bis(dimethylphosphino)ethane
DMPLED:	*N*,*N*′-bis((1,2-dimethyl-3-hydroxy-5-(hydroxymethyl)-4-pyridiniumyl)methyl)ethylenediamine-*N*,*N*′-diacetic acid
DO3A:	1,4,7-tris(carboxymethyl)-1,4,7,10-tetraazacyclododecane
DOTA:	1,4,7,10-tetraazacyclododecane-1,4-7,10-tetraacetic acid
DTPA:	diethylenetetraaminepentaacetic acid
DTPA–BEA:	diethylenetetraaminepentaacetic-*N*,*N*′-bis(ethylamide)
DTPA–BMA:	diethylenetetraaminepentaacetic-*N*,*N*′-bis(methylamide)
DTPA–EOB:	diethylenetetraaminepentaacetic-*N*,*N*′-ethoxybenzyl
EC:	electron capture (radioactive decay)
EC:	*N*,*N*′-ethylene-di-l-cysteine
EDDASS:	*N*,*N*′-bis(2-mercaptoethyl)ethylenediamine-*N*,*N*′-diacetic acid
EDTA:	ethylenediaminetetraacetic acid
h:	hours
HBED:	*N*,*N*′-bis(2-hydroxy-3,5-dimethylbenzyl)ethylenediamine-*N*,*N*′-diacetic acid
HBMA:	*N*,*N*′-bis(2-hydroxy-3,5-dimethylbenzyl)ethylenediamine-*N*-(2-hydroxyethyl)-*N*′-acetic acid
HBPLED:	*N*-(2-hydroxybenzyl)-*N*′-(pyridoxyl)ethylenediamine-*N*,*N*′-diacetic acid
HL91:	4,9-diaza-3,3,10,10-tetramethyldodecane-2,11-dione-dioxime
HP–DO3A:	1,4,7-tris(carboxylmethyl)-10-(2-hydroxypropyl)-1,4,7,10-tetraazacyclododecane
HSA:	human serum albumin
HYNIC:	hydrazinonicotimamide
HYNICtide:	cyclo(d-Val–NMeArg–Gly–Asp–Mamb(5-(6-(6-hydrazinonicotinamido)-hexanamide)))
IT:	isomeric transition
keV:	kilo-electron volts (10^3)
MDR:	multi-drug resistance
Me_4HBED:	*N*,*N*′-bis(2-hydroxy-3,5-dimethylbenzyl)ethylenediamine-*N*,*N*′-diacetic acid
Me_4HBPLED:	*N*-(2-hydroxy-3,5-dimethylbenzyl)-*N*′-((3-hydroxy-1,2,5-trimethyl-4-pyridiniumyl)methyl)ethylenediamine-*N*,*N*′-diacetic acid

meso-EHPG:	*meso*-1,2-ethylenebis(*o*-hydroxyphenylglycine)
meso-TMPHPG:	*meso*-*N*,*N*′-trimethylenebis(2-(2-hydroxy-3,5-dimethylphenyl)glycine)
MeV:	mega-electron volts (10^6)
MRI:	magnetic resonance imaging
NOTA:	1,4,7-triazacyclononane-*N*,*N*′,*N*″-triacetic acid
PCBA:	1-[(1,4,7,10,13-pentaazacyclopentaadec-1-yl)methyl] benzoic acid
PET:	Positron emission tomography
PLED:	*N*,*N*′-dipyridoxylethylenediamine-*N*,*N*′-diacetic acid
PTSM:	pyruvaldehyde-bis(N^4-methylthiosemicarbazone)
rac-EHPG:	*rac*-1,2-ethylene-bis(*o*-hydroxyphenylglycine)
rac-TMPHPG:	*rac*-*N*,*N*′-trimethylene-bis(2-(2-hydroxy-3,5-dimethylphenyl)glycine)
SCN–TETA:	6-[*p*-(isothiocyanato)benzyl]-1,4,8,11-tetraazacyclotetradecane
SESTAMIBI:	2-methoxyisobutaneisonitrile
SHBED:	*N*,*N*′-bis(2-hydroxy-5-sulfobenzyl)ethylenediamine-*N*,*N*′-diacetic acid
SPECT:	Single photon emission computed tomography
t-butyl-HBED:	*N*,*N*′-bis(5-*tert*-butyl-2-hydroxy-3-methylbenzyl)ethylenediamine-*N*,*N*′-diacetic acid
TACN:	triazacyclononane
TACN–HB:	*N*,*N*′,*N*″-tris-2-hydroxybenzyl-1,4,7-triazacyclononane
TACN–HP:	1,4,7-tris(3-hydroxy-6-methyl-2-pyridylmethyl)-1,4,7-triazacyclononane
TACN–MeHP:	*N*′,*N*″-tris(3-hydroxy-6-methyl-2-pyridylmethyl)-1,4,7-triaazacyclononane
TACN–TM:	*N*,*N*′,*N*″-tris(2-mercaptoethyl)-1-4-7-triazacyclononane
TACN–TX:	1,4,7-tris(3,5-dimethyl-2-hydroxybenzyl)-1,4,7-triazacyclononane
Technepine:	[*N*-[2-((3′-*N*′-propyl-3″β-(4-flourophenyl)tropane-2″β-carboxylic acid methyl ester)(2-mercaptoethyl)amino)acetyl]-2-aminoethanethiolato] technetium99m(V) oxide
TETA:	1,4,8,11-tetraazacyclotetradecane-1,4,8,11-tetraacetic acid
Tetrofosmin:	1,2-bis(bis(2-ethoxyethyl)phosphino)ethane
THM$_2$BED:	*N*,*N*,*N*′,*N*′-tetrakis-(2-hydroxy-3,5-dimethylbenzyl)-ethylenediamine
THMBED:	tetrakis-(2-hydroxy-5-methylbenzyl)ethylenediamine
TMAE:	tris(2-methyl(2-propanethiol))aminoethylamine
TRODAT:	[2-[[2-[[[3-(4-chlorophenyl)-8-methyl-8-azabicyclo[3.2.1] oct-2-yl]methyl](2-mercaptoethyl)amino]ethyl]amino] ethanethiolato-(3-)-*N*2,*N*2′,*S*2,*S*2′]oxo-[1*R*-(*exo*-*exo*)] technetium(V),